UNITED NATIONS EDUCATIONAL, SCIENTIFIC AND CULTURAL ORGANIZATION
INTERNATIONAL CENTRE FOR THEORETICAL PHYSICS
I.C.T.P., P.O. BOX 586, 34100 TRIESTE, ITALY, CABLE: CENTRATOM TRIESTE

ICFA INTERNATIONAL COMMITTEE FOR FUTURE ACCELERATORS

ISTITUTO NAZIONALE DI FISICA NUCLEARE INFN

H4.SMR. 394/8

SECOND ICFA SCHOOL ON INSTRUMENTATION IN ELEMENTARY PARTICLE PHYSICS

12- 23 JUNE 1989

Gas Detectors: Recent Developments and Applications

F. SAULI

CERN, Geneva, Switzerland

EUROPEAN ORGANIZATION FOR NUCLEAR RESEARCH

May 1989

GAS DETECTORS: RECENT DEVELOPMENTS AND APPLICATIONS

Fabio Sauli
CERN, Geneva, Switzerland

ABSTRACT

After a survey of the design and operating principles of multiwire proportional chambers, recent developments in the field of gaseous detectors are described and examples of their applications in particle physics and other areas are cited.

Course given at the Second ICFA School on Instrumentation in Elementary Particle Physics, Trieste, 12-23 June 1989
(English version of a course given at the Joliot-Curie School, Maubuisson, France, 25-30 September 1988)

GAS DETECTORS: RECENT DEVELOPMENTS AND APPLICATIONS

Fabio Sauli
CERN, Geneva, Switzerland

ABSTRACT

After a survey of the design and operating principles of multiwire proportional chambers, recent developments in the field of gaseous detectors are described and examples of their applications in particle physics and other areas are cited.

1. INTRODUCTION

In the field of particle physics, today's experimentalists have at their disposal complex and advanced apparatus that enables them to localize and identify events produced by nuclear interactions. A good proportion of these systems use, as detection components, multiwire proportional chambers (MWPCs), which were initially conceived and developed 20 years ago by Georges Charpak and his group at CERN [1]. The MWPCs may take a variety of forms, both flat and cylindrical, with dimensions sometimes exceeding 10 m^2 per component, and, thanks to their excellent time resolution (a few tens of nanoseconds), they work with very good detection efficiency in high radiation fluxes, attaining submillimetric localization accuracy. As they can provide information in digital form, they can be directly connected to complex electronic data recorders. Typical acquisition frequency varies between a few hundred and a few tens of thousands of events per second, depending on the complexity of the recording system.

A quick glance at the situation in nuclear physics at the end of the 1960s should make it possible to appreciate more clearly the considerable impact of this new technology. It was a period of great excitement, due in part to the first quantitative forecasts of models based on quark theory—which, for experimental verification, frequently required the detection of events with an extremely small effective cross-section—and in part to the commissioning of high-energy accelerators with high fluxes. At that time there were basically two types of equipment for detecting events having a complex geometry: i) bubble chambers, which were accurate for determining the topology of interactions but not well suited to the search for rare events because of their non-selective nature, and ii) so-called 'electronic' detectors, made up of spark chambers and of a set of plastic scintillators placed in geometric coincidence, thus making it possible to observe events. The latter method, although selective, had its acquisition rate limited by the dead-times inherent in the gas spark mechanism.

I can still remember the mixed feelings that greeted the first international presentation of the work done using a multiwire proportional chamber, on the occasion of a congress organized at the Chateau of Versailles in 1968: admiration for the attractive operating characteristics (continued sensitivity in high fluxes and the possibility of electronic selection at several decision levels), mingled with perplexity at the prospect of having to use hundreds—if not thousands—of independent electronic channels for amplifying and recording the data.

As a result of a lucky coincidence (not uncommon in scientific research), the beginning of the 1970s was marked by a rapid development in the technology for integrating complex electronic circuitry in one unit; this made it possible to reduce considerably both the cost and the size of the electronics equipping large detectors based on the new technology. At the same time, the general availability of ever more advanced electronic computers made it possible to relax the selection criteria prior to recording on magnetic tape, so that events that were unexpected at the outset could show up during analysis. The development and the use of MWPCs were therefore both very fast and widespread, and is still continuing, as evidenced by the large number of articles on the subject in instrumentation reviews. The use of the new technique is also catching on, albeit more slowly, in other fields such as astrophysics, biomedical research, and structural analysis.

2. PROPORTIONAL CHAMBERS AND DRIFT CHAMBERS

I will limit myself here to a brief description of the main physics processes which make it possible to detect ionizing radiation using proportional counters. The passage of a charged particle or the conversion of a photon in a gas causes a multitude of electromagnetic interactions and can, amongst other things, lead to the appearance of one or more electron–positive ion pairs (a detailed description of the various energy loss processes is given, for example, in Ref. [2]). Primary electrons produced in the gas by these ionizing processes can be sufficiently numerous to be collected and detected directly on appropriate electrodes using a low electric field. High-energy particles, however, produce only a few tens of electrons in the thin layers of gas; for detection, therefore, a multiplication mechanism inside the gas itself has to be used. This process requires the use of high electric fields (10^5 V/cm·atm, or more) usually attained using thin anode wires (thanks to an inversely proportional dependence of the electric field on the distance from the wire). Multiplication in a uniform field is also possible and has certain advantages, as we will see below. As the charge detected depends on the initial charge (although often in a non-linear way), the detector is referred to as 'proportional'.

The structure of the MWPC is shown in Fig. 1. It consists of a plane of thin anode wires, running parallel and situated close together, stretched on an insulating support between two cathodes (sheets, grids, or wires). The application of a potential difference between the anodes and the cathodes, symmetrical in relation to the central [illegible] leads to the appearance of the equipotential field lines shown in the figure. Typical values [illegible]meter of the anode wires and the distance between them are 20 μm and 2 mm, respectively [illegible]e distance between the anode and cathode planes is usually between 5 and 10 mm. The structure [illegible]nsulated from the atmosphere by windows made of thin plastic foils and is filled with a mixture of gases. Although charge multiplication can be achieved in nearly all gases, the choice of the medium is often determined by experimental requirements: for example, a good proportionality, a high multiplication factor, or an efficient gathering of electrons over considerable thicknesses without loss by capture.

The electrons freed in the gas by ionization drift towards the anode wires, close to which, because of the rapid increase in the electric field, they acquire sufficient energy to undergo inelastic and ionizing collisions with the molecules. This leads to the creation of an avalanche of electrons and ions and to the multiplication of the initial charge; the process stops when all the electrons have reached the surface of the anode wires. For detecting and localizing ionizing particles and soft X-rays, moderate proportional multiplication factors are used, typically 10^4 to 10^6, whilst for other applications (for example, shower calorimetry), higher values can be reached (10^7 or more) thanks to the special operating modes. More detailed descriptions of the processes that occur in a proportional chamber are given, for example, in Ref. [3].

In its simplest version, an MWPC has an amplifier–discriminator circuit on each wire, and a digital readout system which makes it possible to record the profile of the wires activated over a given

period. Thus, for each chamber, the projection of the ionizing event on the coordinate axis perpendicular to the anodes is obtained with an accuracy corresponding to the distance between the wires. The second coordinate is provided by another chamber, in which the anode wires are perpendicular to those of the first chamber. The photograph (Fig. 2) shows one of the first large-size MWPCs, with wire-to-wire digital readout, constructed in the beginning of the 1960s [4]. In view of the rapid development in construction techniques and the relative simplicity of the electronic circuits required, digital detectors of this type were amongst the first to be used on a wide scale for high-energy physics experiments.

A better localization accuracy and a true two-dimensionality can be obtained by recording the profile of the signals induced on the cathode plane by the anodic avalanche. A straightforward electrostatic analysis of the charge induced by the avalanche process makes it easy to establish that the major component of the negative signal observed on the anode wire is not the result of the collection of electrons, but of the backward movement of the positive ions produced. This movement induces positive signals on all the adjacent electrodes, as shown in Fig. 3. The two cathode planes consist of fine strips or layers of wires perpendicular to each other, and the profile of the induced charge is measured; both orthogonal coordinates of the avalanche can be calculated in a single MWPC. This method, the so-called 'centre of gravity of the induced-charge' method, makes it possible to obtain a localization accuracy which is sometimes limited only by the intrinsic dispersion of the ionizing track (a few tens of microns for low-energy X-rays).

It should be noted that an almost equivalent accuracy can be obtained for the coordinate parallel to the anode wire and for the perpendicular coordinate—which is, at first glance, surprising. One would expect, indeed, a quantization effect owing to the distance between wires. The accuracy is the result of the remarkable and unsuspected fact that the development of the avalanche, at least at moderate gains, remains well localized around the direction from which the primary electrons originated. The ions produced in the multiplication then go back along the same field lines that lead to the point of origin of the ionization detected. The centre of gravity of the induced signals (calculated using an appropriate transfer function) therefore gives a good idea of the original position. Figure 4 is an example of a two-dimensional image, obtained by irradiating an MWPC with an X-ray source through a stencil of cut-out letters. Each dot corresponds to an event, localized by using the method of centre of gravity of the induced signals [5]. The actual dimensions are shown in the figure. The image is, in fact, detected by a single anode wire over a distance of a few millimetres. The prospects for applying these microradiography methods are remarkable. Some examples will be given below.

Proportional chambers with cathode readout of the type described have been made with various geometries, both flat and cylindrical. The coordinates of the ionizing events are obtained by measuring the charge profile on the cathode strips with analog-to-digital converters. Since the best localization accuracy is attained by using a strip width identical to the distance between the anode and the cathode, a large number of electronic channels are needed, even for a detector of modest size. A detailed study of this localization method is given in Ref. [6].

There are various systems that make it possible to use the cathode information whilst avoiding the electronic complexity of the strip-by-strip readout method, in particular the resistive division of the charge and the serialization of the pulses on electromagnetic delay lines. These simplified systems limit either the localization accuracy or the time resolution, but they are widely used in biomedical research (see, for example, Refs. [7] and [8]).

In the original multiwire chamber, the coordinates of ionizing events are deduced from a measurement of the induced signals, and the time resolution of the apparatus corresponds to the maximum time required for collecting the electrons produced close to the anode wires (usually a few tens of nanoseconds). A measurement of the collection or drift-time of the primary electrons, when

compared with the moment at which the event takes place (for example for charged particles, with an external scintillator), will later provide information on the position of the track. This is the operating principle of multiwire drift chambers (MWDC). Various schemes have been developed to optimize collection characteristics with a view to improving localization accuracy. Since the drift velocity of electrons in gases depends on the electric field, the best results are obtained with an MWDC in which the field is constant over the greater part of the trajectory. Figure 5 gives an example [9]. The anode wires are centred in a symmetrical drift cell where the electric field is created by two networks of cathode wires, with the potential decreasing on either side of the anode. The resultant equipotential lines are shown in the figure. The limits between adjacent cells are set by a further cathode or field wire. The electric field and, as a result, the drift velocity of the electrons are constant in most of the cell (except for the region next to the anode wire where multiplication takes place). Several elementary drift cells, such as the one shown in the figure, can be used to form a larger chamber. Each anode wire is fitted with a time-measurement circuit or a digital converter. The left-right ambiguity inherent in this structure is resolved by having several chambers placed out of phase in an appropriate way, or by a couple of closely adjacent anode wires in place of the single wire shown in the figure.

The localization accuracy of an MWDC depends on a number of systematic or dispersive factors. The intrinsic limit is determined by three main elements: the diffusion of electrons as they pass through the gas; the primary production statistic, i.e. the average distance between the groups of electrons produced by ionization; and the electronic dispersion in the drift-time measurement. These elements are indicated in Fig. 6, which shows a typical localization accuracy measurement for high-energy charged particles as a function of the distance from the anode. The average accuracy is close to 50 μm. A greater degree of accuracy can be obtained by working under high pressure, which reduces dispersion caused by diffusion and increases the density of primary ionization.

Large-size drift chambers that provide more modest localization accuracies than the one we have mentioned have been made at CERN, for example for large neutrino detectors.

3. VOLUMETRIC DRIFT CHAMBERS

The multiwire chambers that have just been described are thin structures with a large surface area in which ionizing tracks are measured once. Events with complex geometry require a great number of independent measurements over the track length, and therefore many detectors in line. Another way of establishing the topology of interactions is to use a large amount of gas as a detector, with the ionizing electrons drifting to a single, thin MWPC placed at one end of the gas volume. Chambers of this type give an image or a time projection (Time Projection Chamber, TPC). Thanks to their large size, the TPCs make it possible to produce a very accurate picture of the ionizing tracks with a limited number of measuring channels. Apart from the drift-time, they also measure the pulse height of each segment of the track, and they can identify, within certain limits, particles in the region of momentum at which the differential energy loss depends on speed.

Imaging chambers of different sizes and with different geometries have been built; for experiments inside accumulator rings the cylindrical shape is preferred. Examples of large-volume detectors of this kind are the Berkeley TPC used at Stanford, the JADE detector at DESY, Hamburg, and ISIS and the central detector of the UA1 at CERN. Review articles on these detectors and other instruments of the same type are contained in Ref. [10].

Designed in the 1970s by D. Nygren and his team at Berkeley [11], the TPC is perhaps the most sophisticated example of this type of detector; it consists of a large drift volume with a uniform electric field. The electrons produced in the sensitive volume drift to the multiplying part — a MWPC with signal readout on the anode wires and on strips of small pads on the cathode layer. An example of a TPC is shown in Fig. 7 [12].

This type of detector has been adopted by many researchers, in particular for the ALEPH and DELPHI experiments being prepared at the CERN Large Electron-Positron collider (LEP). Figure 8 shows the ALEPH TPC being fitted. Because of the great size of the detector, the MWPC in the front end is assembled from modular components.

Figure 9 shows a simulated event as detected and reconstructed in the ALEPH TPC; the detector's power of analysis for complex events is clear.

When interaction rates are very high, the long drift-time of a TPC (several tens of microseconds) becomes intolerable. The detector is then split into a number of drift modules of more modest size. The large UA1 detector at CERN, with which the intermediate bosons were discovered, is an example of such a detector (Fig. 10) [13].

Each module, shaped as a cylindrical section, has a conversion and drift area in which the ionized track is formed, and a multiwire chamber at one end for multiplication and detection (Fig. 11). As in most detectors of this type, the sensitive volume consists of alternating anode and field wires, which, in addition to improving the uniformity of the multiplying field, also reduce the mutual induction between the neighbouring anode wires. Each of the modules records the drift-time and the pulse width of the track segments at both ends of the anode wire (selected with a high resistivity). The relationship between the charge-signal amplitudes at the two ends of a resistive wire gives the longitudinal position of each track segment. To analyse the momentum of the charged particle, the detector is inserted in the magnetic field created by a dipole magnet with a cylindrical gap. Figure 12 shows an example of a complex event, recorded using the detector described, as it appears on the computer screen used for the acquisition and analysis of data. Each dot shows part of the track measured. Other information, such as the pulse height recorded on the calorimeter components, is also shown.

The localization accuracy obtained with this type of chamber depends mainly on the accuracy with which the function of the correlation between the drift-times measured and the real position of the track is known. This function is particularly complex when there are magnetic fields that lead to considerable distortions in the trajectories of drifting electrons. It should be noted that it is possible to minimize such effects by building a detector in which the electric and magnetic fields are parallel (the lateral deflection of the electrons is then zero). The Berkeley TPC is an example of this configuration.

As the examples mentioned show, volumetric drift chambers are powerful tools for determining the topology of complex events. The main limitation of their use is the drift-time of the electrons (a few microseconds) and the collection-time of the ions generated during the multiplication process (a few milliseconds). A high flux can lead to an overlap of events and distortions of the electric field, which may perturb the drift trajectory of the ionized track. The reason for splitting up the UA1 detector into a large number of modules of reduced drift thickness is precisely to limit such effects.

4. IDENTIFICATION OF CHARGED PARTICLES

The detectors described above enable us to reconstruct, with optimal accuracy, the geometry of complex events, and when embedded in a magnetic field, they provide us with the momentum value of each of the charged tracks. To identify the particles, an independent kinematic value must be measured: energy, mass, or speed.

4.1 Measurement of the differential energy loss

The energy lost by charged particles in thin layers of gas depends, as we have seen, on their speed. Because of the large dispersion inherent in the process, hundreds of separate measurements are needed to provide a good estimate of average loss. This can be achieved using the drift chambers

described above as they record the pulse height on each anode wire. An example of the resolution given by this method with the Berkeley TPC is shown in Fig. 13 [14]. Different masses that are clearly separated in the low-momentum zone can still be identified within the limits of statistical analysis in the region above a few GeV/c (thanks to the slight relativistic rise in energy loss).

4.2 Cherenkov ring detectors

This method is only mentioned briefly in passing; a detailed discussion can be found, for example, in Ref. [15].

The recent development of multiwire chambers capable of high gains in a mixture of photosensitive gases has made it possible to capitalize on another physical property of fast particles to help identify them. Let β be the speed of a particle (in relation to the speed of light) and n the refractive index in a transparent medium; if the relation $\beta < 1/n$ is satisfied, photons are emitted by Cherenkov effect at an angle of $\Theta = \arccos(1/\beta n)$ in the direction of the movement. This cone of light, reflected by a spherical mirror with radius R_{mir}, forms a circle with radius $r = (R/2)\tan\Theta$ in the image plane; thus the measurement of the radius of the ring gives the speed of the particle (Fig. 14). Photons are emitted by Cherenkov effect over the entire frequency range, but they can of course only be detected in the range for which the radiator is transparent. At high energy, where gas radiators with a low refraction index have to be used, only a small number of photons can be detected for each track, usually around four or five. The identification method described above, which involves the localization of isolated photons, was demonstrated several years ago using electronic image amplifiers that were sensitive to visible wavelengths; however, this method was rarely used because of its very limited acceptance. With the development of photosensitive proportional chambers, the technique can be used in experimental set-ups with a large solid angle. As there are no gases with an ionization threshold in the visible wavelength, detection is carried out in ultraviolet light, after having chosen the appropriate radiation medium and the type of window for separating the radiator and the detector [16]. It should be noted that the quantum efficiency of the gases above the ionization threshold may be very high (50% to 60%), as against 10% to 20% for a traditional photocathode.

The first work using Ring-Imaging Cherenkov (RICH) chambers were carried out using triethylamine (TEA) vapour as the photosensitive product with an ionizing potential of 7.5 eV (therefore in the far ultraviolet range), which means that windows made of calcium fluoride, which is transparent to photons with an energy of up to about 10 eV, had to be used. Recently, a vapour with an even lower ionization potential (5.4 eV) has been found: tetrakis(dimethylamine)ethylene (TMAE). By employing TMAE as the photosensitive product, quartz windows transparent to 8 eV can be used, the advantage being that they are much sturdier and cheaper than the ones made of fluoride crystals. More important—when working at wavelengths closer to that of visible light—there is a greater choice of radiant media. The main disadvantage of TMAE is its low vapour pressure at ambient temperature (a fraction of a torr) which means that conversion thicknesses of several centimetres have to be used to ensure reasonable efficiency. The result is a time resolution of a few microseconds, and consequently a major limitation of the maximum flux permissible without causing confusion. The alternative, which is riddled with obvious technological difficulties, is to heat the detector to around 60 °C to 70 °C to increase the TMAE concentration.

The actual construction of a particle identifier based on these principles depends mainly on the capacity to detect and localize, in a multiwire chamber, individual photoelectrons produced in the gas. This implies operation at high gain (10^5 or more) in a photosensitive gas, and is especially apt for producing secondary phenomena caused by the emission and reconversion of photons during the avalanche multiplication process. In a conventional MWPC, these processes appear at gains above 10^4, and often lead to an instability or discharge regime. A solution proposed and used by our group

is based on a variant of the MWPC, the Multistep Proportional Chamber (MSPC [17]), which uses a parallel-plate preamplifier element (see Fig. 15). A set of parallel, semitransparent metal grids, to which the appropriate potentials are applied, cordons off three regions of the electric field above a conventional proportional chamber. In the first of these regions—the conversion volume, which is in contact with the input window—the ultraviolet photons emitted by the radiator ionize the molecules of the photosensitive vapour. The photoelectrons produced as a result reach the second region, which has a very high field, where they multiply by avalanche by a factor of around 10^4. A fraction of the electrons created by the avalanche (around 10%) then enter the third area (transfer volume) and continue towards the MWPC, where amplification and detection take place in accordance with the process described before. As the two amplification structures are almost independent, very high combined gains, close to 10^7, can be attained without secondary limiting phenomena [18].

Figure 16 shows an example of a Cherenkov ring that was obtained by superposing, on the cathode screen of a computer, about 100 events generated by a monoenergetic and collinear beam in an instrument of the type described. Each event includes an average of five detected photons. We have built an experimental set-up that is capable of identifying particles in a momentum range between a few tens and a few hundreds of GeV/c, and we have put it into operation at Fermilab in collaboration with other research institutes.

Figure 17 shows the most delicate component in this apparatus: the calcium fluoride window that separates the radiator (helium at atmospheric pressure) from the photosensitive chamber. The window must, of course, be impermeable to the photosensitive vapour molecules, and must be able to resist any mechanical stress and thermal dilation that could cause the crystals to crack. Figure 18 shows the computer-reconstructed image of a Cherenkov ring defined by five detected photons. It should be noted that the radius can be measured with a single photon, as the trajectory of the charged track is known once it has been measured by the proportional chambers used for momentum analysis, and as the centre of the ring is clearly established. The resolution obtained during the experiment is shown in Fig. 19. The particles π and K are well identified over the whole momentum range [19].

High gains can be obtained in photosensitive mixtures with detectors whose geometry minimizes the secondary effects caused by photons emitted during the avalanche. This can be done, for example, by encasing each anode wire in a cathode made up of a fine metal tube, with a longitudinal window close to the conversion region. The potentials are chosen in such a way as to guide the photoelectrons most efficiently to an amplifier wire; moreover, the wire reduces the reconversion, in the gas, of the secondary photons emitted in the avalanche (these are absorbed by the cathode). For the conversion and detection of Cherenkov photons where a fast time resolution is not necessary, a geometry similar to that of the TPC [15, 16] can be used. The photoelectrons produced in the gas drift in the uniform field to the amplification region, made, for example, in the way described above. Measurement of the drift-time on the anode wires provides the coordinates of the conversion points. A large Cherenkov ring imager is being made at CERN for the DELPHI experiment. As a result of using TMAE as the photosensitive product, which makes it possible to choose from a wide selection of radiators, the apparatus reaches optimum identification power in a large range of momenta and covers most of the solid angle around the LEP intersection region. The time resolution, and therefore the rate capability, is of course limited by the long drift-time (around 20 μs for the quoted detector).

4.3 Other methods of particle identification

I will briefly mention two other systems that make considerable use of proportional chambers for identifying fast particles. The first of these systems is based on detecting what is referred to as 'transition radiation', i.e. the emission of high-energy photons (usually soft X-rays) by relativistic

particles as they pass across the interface between two materials with different dielectric constants. The spectrum of photons emitted shows a pronounced peak at an energy level depending on γ, the Lorentz factor of the particle, and their number increases rapidly with speed. As the probability of emission by interface is low, a packet of several hundred sheets of a light material (polyethylene, lithium) must be used as the radiator, separated by thin gaps to minimize the auto-absorption of photons. In this way it is possible to detect them with great efficiency, using one or more proportional chambers in the soft X-ray range and with xenon as the filling gas. The identification power improves as γ increases, in contrast to what happens for Cherenkov ring imaging and when the differential energy-loss method is used (in which saturation is reached at relativistic energy).

A second method of identification, used for charged or neutral radiation, is the calorimetry method. It consists basically of converting all the energy of the projectile into a detectable signal by alternating layers of dense material and components for measuring the ionization produced by showers in the gas. Although conventional proportional chambers can be used as ionization detectors, there is another apparatus, developed by Iarocci and his collaborators [20], which makes it possible to have large sensitive areas for a reasonable price: this device is composed of limited streamer tubes. Each sensitive component consists of an anode wire stretched across the centre of a plastic element having a square cross-section, and which is coated on the inside with a graphite conducting layer. Numerous adjacent but separate cells can be constructed over a distance of several metres using extruded plastic. Because of the high surface resistivity of the cathodes, and by using anode wires with a large diameter (50 to 60 μm), it is possible to pass beyond the proportional operating region to reach that of the limited streamer. With a multiplication factor of around 10^7–10^8 this operating regime has the advantage of allowing direct detection without amplifiers and of producing the same pulse height regardless of the primary ionization. This is particularly interesting for calorimetry; in fact, the signal recorded by the detector depends on the total number of tracks in the shower rather than on their energy loss. The dispersion caused by the emission of slow electrons, which are heavily ionizing, is therefore kept to a minimum. The first large streamer-tube calorimeter was made for the experiment to determine the lifetime of protons, which was installed in the Mont Blanc tunnel where it is still in use. Other similar systems are being made for various experiments, including some at LEP.

5. IMAGING CHAMBERS

All the detectors described so far have one characteristic that they use electronic readout of signals to extract information. It has been known that under certain conditions, photons are also emitted in large quantities by electron avalanches, and that they can be detected by using the appropriate methods—photomultipliers or other means. The emission of photons is particularly abundant in pure noble gases, and this gave rise to the family of proportional scintillation counters; for a review, see Ref. [21].

This type of counter, with very good energy resolution, has, however, a very modest space resolution, corresponding to the size of the photomultiplier; readout methods using several tubes are possible, which allows for an interpolation, but they are limited in the case of single avalanches.

With the availability on the market of optical captors with high granularity [such as solid-state cameras or charge-coupled devices (CCDs)] and of rapid image-digitization systems, it became clear that a light-emitting detector could be used; all that would be necessary, for example, would be to examine the plane of a proportional chamber with a camera to observe the images of events that occur—even complex ones. There is, however, one major problem: inert gases emit photons in the far ultraviolet range (150 nm for argon), which would mean that calcium fluoride or magnesium fluoride windows would have to be used. Moreover, scintillation efficiency is considerably reduced

by the presence of pollutants, even if they are present in only tiny quantities. Recently, in the course of the research into the photosensitive gases used to detect photons, it was discovered that the addition of different vapours, such as TEA and TMAE, to noble gases shifts the scintillation wavelength into the visible range (280 nm for TEA and 490 nm for TMAE) [22–24]. These wavelengths can pass through plastic windows (Aclar, for example, is transparent above 220 nm); scintillation would then be detected by a system made up of a light amplifier coupled with a solid-state camera and a video digitizer.

Figure 20 shows an example of an image recorded using this method, with a small chamber of the TPC type exposed to cosmic rays. It was found that the best light-yield in an imaging chamber is achieved by using a parallel-plate avalanche chamber (instead of the multiwire type) as the scintillation element; this offers obvious practical advantages.

Measurement of the light emitted by avalanches gives information on energy loss; Fig. 21 shows, for example, the digital representation (in shades of grey) of the interaction of an α-particle in helium, recorded with an imaging chamber [25]; the numbers indicate the integral light intensity on each segment, and the energy balance is that corresponding to the reaction. If one considers that the real length of the primary track is around 3 cm, the power of the imaging chamber for reconstructing complex events is obvious.

Several applications of the imaging chamber have already been studied; I shall describe two of them: one for Cherenkov imaging, and one for electromagnetic calorimetry.

5.1 The imaging chamber for detecting Cherenkov rings

In the previous section, I mentioned that one of the limits of the electronic methods used in detecting Cherenkov rings was the difficulty in accurately reconstructing events consisting of a large number of photons or multiple tracks. It is clear that the optical method, which is truly two-dimensional and has a number of resolution elements that would be very difficult to produce electronically (usually 500 × 500 pixels), is not hindered by any such limitations. A prototype of a Cherenkov imager based on an imaging chamber has recently been developed [23, 26]. The detector is a multistep chamber, capable of high gains, with a pulsed gate at the end of the drift region for selecting events (Fig. 22). The last gap in the chamber—a parallel-plate element—generates the image, which is then analysed by the light amplifier. It was decided to operate the detector at low pressure to reduce the influence of direct losses, by ionization, of the charged particles passing through the chamber; this also makes it possible to achieve a high gain in the mixture containing TMAE.

Figure 23 gives an example of a Cherenkov ring, recorded with the imaging chamber in a beam of fast charged particles; the average number of clusters (each one corresponds to a photon detected) is 10, and the localization accuracy (estimated by calculating the centre of gravity of each track) is around 2 mm.

The same type of detector can be used to see photons emitted by the Cherenkov effect in a solid or liquid radiator in which an electromagnetic shower develops. The shape and the position in the plane of the image make it theoretically possible to deduce the angle of incidence of the gamma, which is at the origin of the shower [27]. An example obtained with a multistep chamber operating at atmospheric pressure is shown in Fig. 24 [28].

5.2 The high-density imaging chamber for electromagnetic calorimetry

Conventional gaseous chambers do not lend themselves directly to the detection of hadronic or electromagnetic showers because of their low mass. However, such chambers have been used as the sensitive component in sampling calorimeters, alternating with heavy conversion layers. An even

better approach is that of the high-density projection chamber, developed initially by Charpak and his collaborators for detecting 500 keV gammas for a positron camera [29] and since adopted by several experimentalists for shower detection [30]. These chambers contain a conversion region made up of thin metal plates, parallel and insulated from one another, with open channels in the gaseous medium and with potentials allowing the collection and drift of ionization electrons towards the multiplication element (a MWPC). The energy resolution of this detector, called a high-density proportional chamber (HPC), is very good, but the localization properties are limited by the usual problems of electronic resolution.

We made an HPC imaging chamber by replacing the proportional chamber with an avalanche chamber detecting the light emitted [31]. Two examples of the images obtained with a prototype are shown in Fig. 25: at the top, the development of an electromagnetic shower, and at the bottom, a hadron interaction. The difference between these two types of interaction is striking and illustrates the power of the imaging chamber.

Of course, the imaging chamber, although unbeatable where granularity is concerned, suffers from a serious limitation when it comes to the digitization and recording of data. Commercially available systems, based on the television standard, have acquisition rates limited to 50 Hz; special components can probably operate at a few hundred images per second. However, one should take into account that this limit applies only to the image acquisition system; the chamber itself is as fast as a conventional proportional chamber. Moreover, by using a multistep structure, one can exploit the delay in the gas, which makes it possible to select data for good events only; the chamber and the light amplifier can be activated by a command from an external pulse. This makes it possible to consider using imaging chambers in high-flux conditions.

6. APPLICATIONS OF PROPORTIONAL CHAMBERS IN OTHER FIELDS

Since they were first developed, proportional chambers have been used outside the field of particle physics as radiation detectors with applications in biophysics, medical research, and astrophysics. Their operating characteristics, which permit fast data acquisition, make them suitable tools for use in advanced research in a number of areas. However, in view of their relatively complicated operation (which involves, for example, a gas circulation system), diagnostic systems based on MWPCs are still considered to be in the experimental phase.

Here I shall limit myself to describing three applications in the above-mentioned areas, chosen from those in which I have been directly involved.

6.1 Radiography by nuclear diffusion

The first application — fast-proton radiography — is the one which comes closest to the domain of particle physics. It is based on a simple nuclear diffusion experiment in which interacting tracks and fragments issuing from the collision are detected in a series of thin MWPCs. Trajectory analysis makes it possible to reconstruct the vertex of the interaction and to deduce, on the basis of the space distribution of the interaction points, the photographic density of the object being analysed; in medical parlance, this is known as three-dimensional tomography [32]. The main feature of this method, compared with that of X-ray tomography [using the computer-aided tomography (CAT) scanner] is that it does not have preferred measuring planes, and that the whole of the densitometric image is captured in one single exposure. Moreover, it is possible to make radiographs of very dense and thick solid objects, such as uranium ingots, which are opaque to X-rays, thus opening the way to a number of applications of industrial interest. Figure 26 shows an example of the tomography of an electric motor carried out at CEN-Saclay. Thanks to the data-acquistion speed of the apparatus (around 100,000 events per second), it is possible to perform dynamics studies directly, or to synchronize data-taking with a given phase of motor rotation.

6.2 Two-dimensional maps of radioactive tracer elements

Most biological preparations can be marked selectively by using radioactive tracer elements that emit β electrons with energies varying between a few keV and a few MeV. Certain isotopes, for example ^{3}H, ^{14}H, ^{32}P, and ^{131}I, can replace the corresponding atoms of a molecule; a one- or two-dimensional map of their distribution will give information about the composition of the preparation (using methods that are similar to conventional chromatography). As they are heavily ionizing, the electrons emitted are easy to detect and localize with a proportional chamber. As each disintegration is individually recorded, a detector of this type is not subject to the limitations inherent in photographic methods, i.e. a limited dynamic range and a long exposure time. Dynamic phenomena can also be studied by recording data as a function of time. Moreover, the possibility of having data in digital form also makes it possible to apply mathematical filtering procedures in order to increase the contrast and to give a stochastic character to the noise. Figure 27 [33] shows an example of digital autoradiography carried out by a group from the University of Pisa on a few monocellular layers, marked with tritium and placed on a flat support a few millimetres away. The activity distribution is shown in the top part of the figure, before and after the application of a mathematic noise-reduction filter (the white indicates the maximum count). In the lower half of the picture a projection on the horizonal axis and an isometric distribution of the activity can be seen. This apparatus is used when studying the faulty reconstruction of mutant cells damaged by ultraviolet rays. As the method is not destructive, the cellular colony can multiply after the measurement.

Obtaining high-resolution images of compounds that are marked by using high-energy electron emitters (^{14}C, for instance) does, however, pose a problem because of their range in the detector gas. We solved this problem by using a variant of the multistep chamber described above. If we go back to Fig. 15 and remove the conversion area, the radioactive preparation to be studied is either placed directly on the second electrode or is seen through a thin gas-tight window placed on this electrode. The electrons emitted in the field can cross the whole structure at various angles, leaving an ionized track. Thanks to the exponential avalanche multiplication characteristics in the preamplification volume, only the first parts of the track, i.e. those closest to the point of emission, are fully amplified and localized. One therefore obtains submillimetric localization accuracy despite the fact that the electrons emitted by the marker have covered a path of several centimetres in the gas [34]. The same apparatus has been used to localize thermal neutrons interacting in a sheet of gadolinium placed directly on the preamplifying electrode. The electrons emitted by internal conversion have an average energy of 70 keV and would not give good localization in a conventional proportional chamber [35].

6.3 Study of crystalline structure using X-ray diffraction

The diffraction pattern of monoenergetic X-rays on crystals depends, as we have already seen, on their electronic configuration. Many proteins and organic macromolecules can, because of their particular structure, be obtained in crystalline form and analysed using the method suggested. However, given the complexity of their structure, the diffraction spectra usually have to be detected over several hundred exposures, and at various angles and energies. This is done not only for the original molecules but also for molecules in which certain atoms, situated at specific points, have been replaced by metals whose absorption lines lie in the range of energy of the X-rays used. With the creation of specialized research centres, and by making use of the synchrotron light emitted by an electron accelerator, highly collimated monoenergetic X-ray beams have become available; fast electronic detectors such as the proportional chamber have made it possible to do such measurements automatically. I shall now describe a particular detector—the spherical proportional chamber—which was built at CERN, and which has been in use for some time at the Laboratoire de l'Accélerateur Linéaire (LAL) in Orsay.

As we saw in the Introduction, the multiwire proportional chamber is well suited to the localization of soft X-rays. But for an energy of 8 to 10 keV, good detection efficiency can only be obtained with considerable conversion thicknesses. In the case that is of interest to us, i.e. wide-angle diffraction on a crystal, a flat conversion structure would lead to a major paralliax error (as there is no means of measuring the penetration of the photons converted in the gas). This problem is solved by organizing a conversion and drift region with a radial field structure, which is centred on the crystal using electrodes with a spherical cross-section. The charges produced by photoionization in the direction of the field are channelled towards the flat detection structure formed by a conventional MWPC [36]. The photograph (Fig. 28) shows the apparatus during data-taking at Orsay; the collimated X-ray beam strikes the crystal mounted on a goniometer, and the two-directional diffraction spectrum is detected by the chamber, which can be seen on the right of the photograph. The data collected by the acquisition system are recorded on tape for subsequent analysis in order to determine the position and the intensity of the reflections for a large number of angular positions of the crystal—information which later serves to establish the structure of the macromolecule. Figure 29 shows an example of an electronic structure obtained using this apparatus. The protein that was analysed has a mass of around 10,000 amu [37].

Thanks to the data-acquistion speed and to the development of semi-automatic calculation algorithms, it was possible to analyse structures in a few days—not many years ago, this would have required months of work.

6.4 Industrial radiography

For industrial applications, it is worth finding ways of making proportional chambers effective for detecting hard X-rays of a few hundred keV. One method, the high-density proportional chamber or HPC, has already been described, but it is far too complicated and costly to be of interest commercially as a widely available tool.

Recently, a group working for the Schlumberger company has developed quite a stylish alternative method of solving the problem [38]: it makes use of a conventional proportional chamber, with a cathode consisting of a metal conversion sheet that is sufficiently thin (a few hundred microns) to allow the photoelectron, produced by an X-ray conversion to escape and to ionize the gas in the chamber. The idea is to get the X-ray beam to hit the conversion sheet at a very small angle, which of course reduces the angular acceptance but increases the efficiency. The generator-detector unit then moves in relation to the object in order to take the radiograph. An example of the image obtained (in a few minutes) by scanning a car is shown in Fig. 30.

7. SUMMARY AND CONCLUSION

We have done our best in these few notes to describe the functioning and the main operating principles of multiwire proportional chambers and various other structures that have originated from them. The examples of design and application given are far from exhaustive. Moreover, research under way indicates that further progress will soon be made, both as regards construction techniques and as regards simplicity, reliability, and operating characteristics. These instruments which are widely used today as detectors in particle physics, are arousing increasing interest amongst experimenters working in other areas of research.

REFERENCES

[1] G. Charpak, R. Bouclier, T. Bressani, J. Favier and Č. Zupančič, Nucl. Instrum. Methods **62** (1968) 235.

[2] L.G. Christophorou, Atomic and molecular radiation physics (Wiley, New York, 1971).

[3] F. Sauli, Principles of operation of multiwire proportional and drift chambers, CERN 77-09 (1977).

[4] G. Charpak, G. Fischer, A. Minten, L. Naumann, F. Sauli, G. Flügge, Ch. Gottfried and R. Tirler, Nucl. Instrum. Methods **97** (1971) 377.

[5] G. Charpak, G. Petersen, A. Policarpo and F. Sauli, Nucl. Instrum. Methods **148** (1978) 471.

[6] G. Charpak and F. Sauli, Annu. Rev. Nucl. Part Sci. **34** (1984) 285.

[7] V. Perez-Mendez, IEEE Trans. Nucl. Sci. **NS-23** (1976) 1334.

[8] F. Sauli, Proc. 2nd Int. Conf. on Application of Physics to Medicine and Biology, Trieste, 1983 (World Scientific, Singapore, 1984), p. 273.

[9] A. Breskin, G. Charpak, F. Sauli, M. Atkinson and G. Schultz, Nucl. Instrum. Methods **124** (1975) 189.

[10] Proc. Workshop on the Time Projection Chamber, Vancouver, 1983 (Amer. Inst. Phys. Conf. Proc. 108, New York, 1984).

[11] A.A.L. Clark et al., Proposal for a PEP facility based on the Time Projection Chamber PEP-4 (1976).

[12] F. Snider et al., Nucl. Instrum. Methods **A268** (1988) 75.

[13] M. Barranco Luque et al., Nucl. Instrum. Methods **176** (1980) 175.

[14] H. Aihara et al., IEEE Trans. Nucl. Sci. **NS-30** (1983) 63.

[15] T. Ypsilantis, Phys. Scr. **23** (1981) 370.

[16] J. Séguinot and T. Ypsilantis, Nucl. Instrum. Methods **142** (1977) 377.

[17] G. Charpak and F. Sauli, Phys. Lett. **78B** (1978) 523.

[18] R. Bouclier et al., Nucl. Instrum. Methods **205** (87) 403.

[19] M. Adams et al., Nucl. Instrum. Methods **217** (1983) 237.

[20] E. Iarocci, Nucl. Instrum. Methods **217** (1983) 30.

[21] A. Policarpo, Space Science Instr. **3** (1977) 77.

[22] M. Suzuki, P. Strock, F. Sauli and G. Charpak, Nucl. Instrum. Methods **A254** (1987) 556.

[23] G. Charpak et al., IEEE Trans. Nucl. Sci. **NS-35** (1988) 237.

[24] D. Sauvage, A. Breskin and R. Chechik, Weizmann Inst. preprint WIS-8818 (1988).

[25] G. Charpak et al., Nucl. Instrum. Methods **A269** (1988) 142.

[26] A. Breskin et al., IEEE Trans. Nucl. Sci. **NS-35** (1988) 404.

[27] Y. Giomataris and G. Charpak, preprint CERN-EP/88-94 (1988), presented at the 20th Int. Cosmic-Ray Conf., Moscow, 1987.

[28] Y. Giomataris et al., preprint CERN-EP/88-96 (1988), presented at the Int. Conf. on Advanced Technology and Particle Physics, Como, 1988.

[29] A. Jeavons, G. Charpak and R. Stubbs, Nucl. Instrum. Methods **124** (1975) 591.

[30] H. Fisher and O. Ullaland, IEEE Trans. Nucl. Sci. **NS-27** (1980) 38.

[31] P. Astier et al., IEEE Trans. Nucl. Sci. **NS-36** (1989) 300.

[32] G. Charpak and J. Saudinos, Progr. Nucl. Med. **7** (1981) 164.

[33] R. Bellazzini et al., report INFN/TC-82/1 (1982).

[34] G. Petersen, G. Charpak, G. Melchart and F. Sauli, Nucl. Instrum. Methods **176** (1980) 67.

[35] G. Melchart, G. Charpak, F. Sauli, F. Petersen and J. Jacobe, Nucl. Instrum. Methods 186 (1981) 613.
[36] R. Kahn, R. Fourme, R. Bosshard, B. Caudron, J.C. Santiard and G. Charpak, Nucl. Instrum. Methods **201** (1982) 203.
[37] R. Kahn et al., FEBS Letters **179** (1985) 133.
[38] J. Dorion et al., IEEE Trans. Nucl. Sci. **NS-34** (1987) 442.

* * *

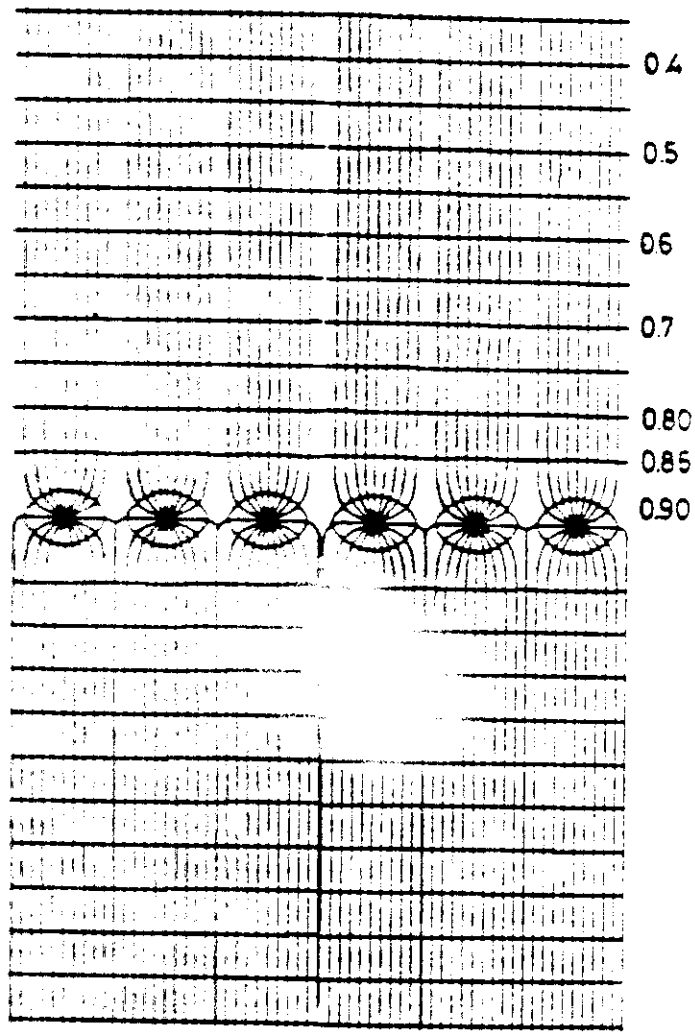

Fig. 1 Construction diagram and map of the electric field in a MWPC. A plane of thin anode wires is stretched between two cathode planes. The application of a symmetrical potential difference leads to the formation of equipotentials and field lines, as shown. The electrons, produced by ionizing events in the filling gas, drift towards the anodes and multiply by avalanche in the high field.

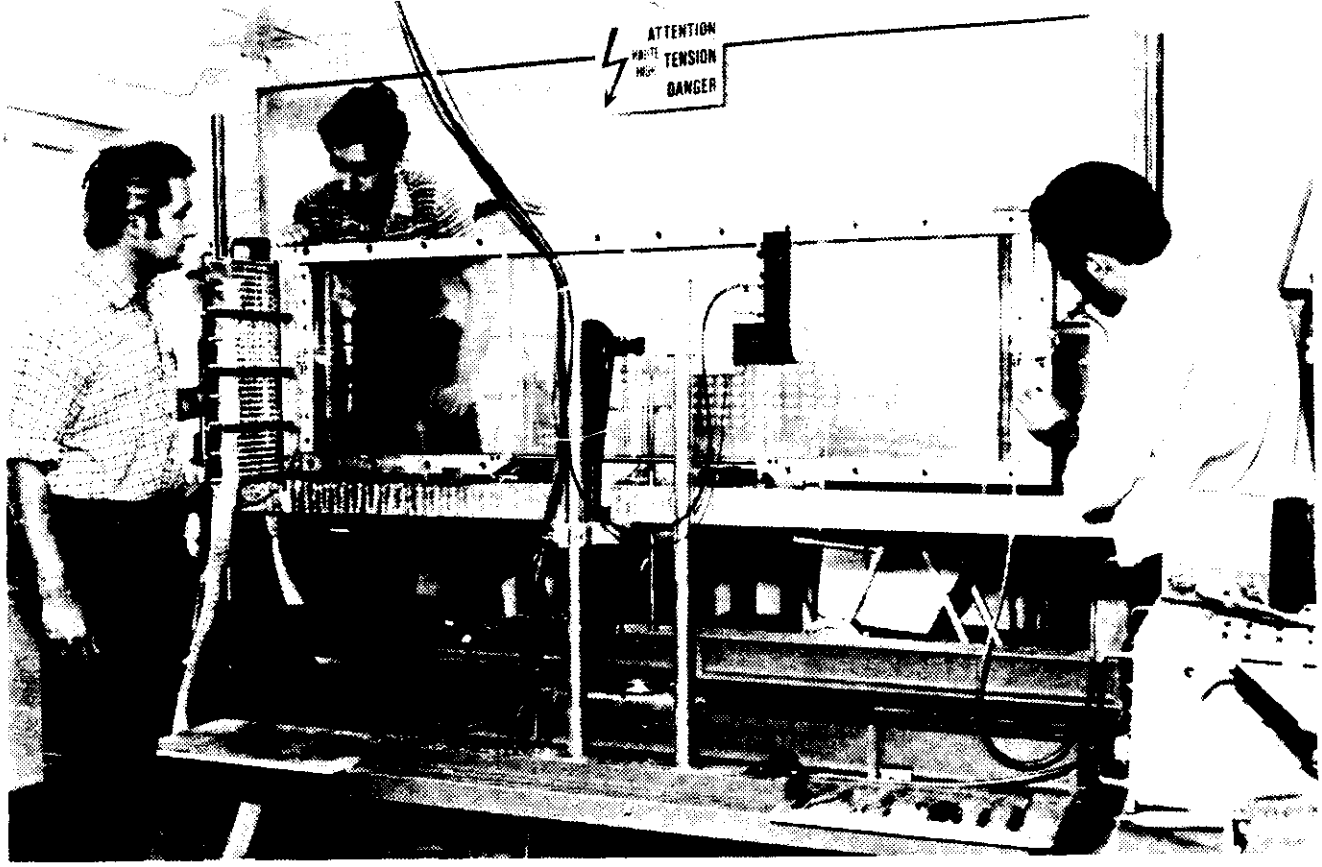

Fig. 2 One of the first multiwire proportional chambers built at CERN at the beginning of the 1970s. On the left is Georges Charpak, with, to his right, the author.

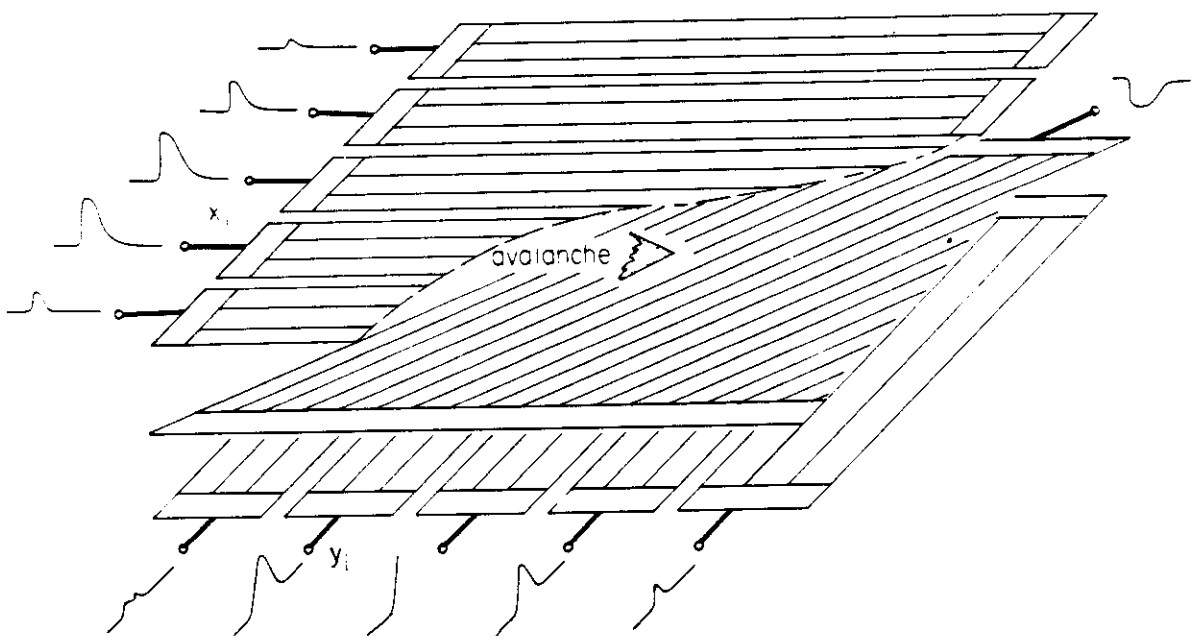

Fig. 3 The charge avalanche that develops in the multiplication process on the anodes induces a negative signal on the given anode wire and positive signals on all the electrodes surrounding it. A measurement of the profile of the charges induced on the cathode planes makes it possible to obtain two- dimensional coordinates for the event.

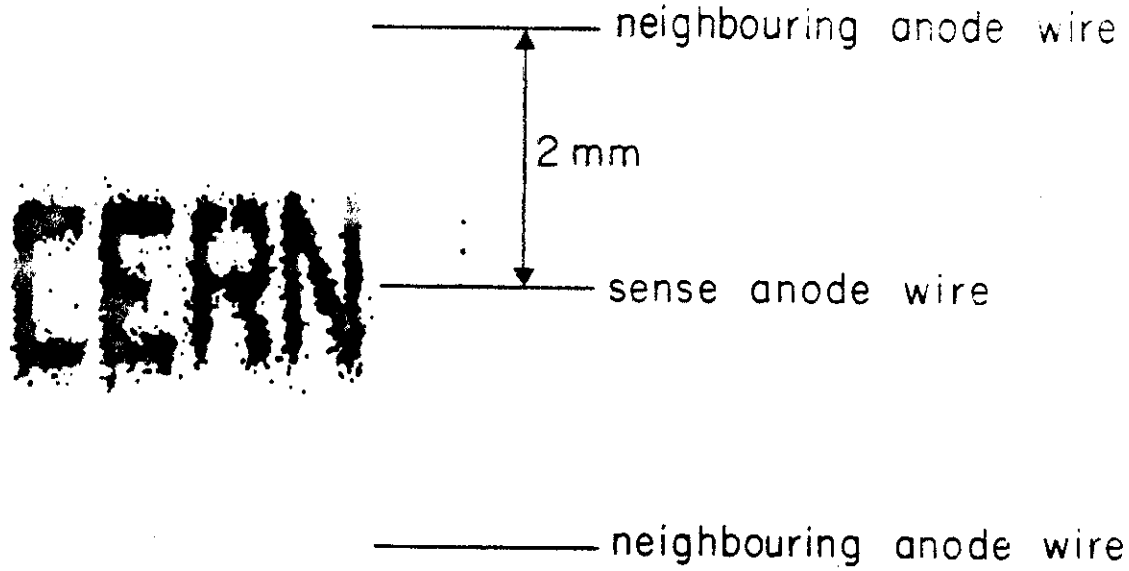

Fig. 4 An example of the localization accuracy that can be reached using the induced-charge method. The image is obtained by irradiating the proportional chamber with an X-ray source through a collimator system. Each dot shows a measurement of position; the external dimensions of the acronym are 4 mm by 2 mm.

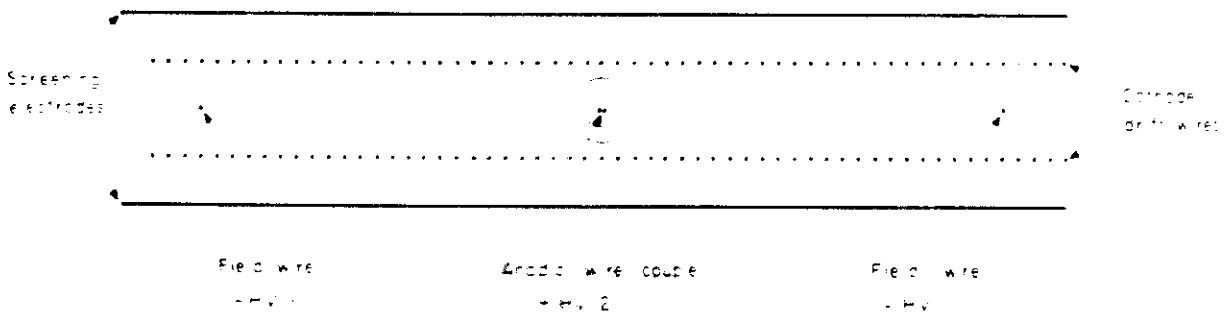

Fig. 5 Example of a drift chamber. The appropriate layout of cathode wires with different potentials makes it possible to create a uniform electric field in which the electrons, produced in the gases by ionization, drift toward the anode wires, where they are multiplied and detected. A measurement of the drift-time provides the distance of the track from the wire directly.

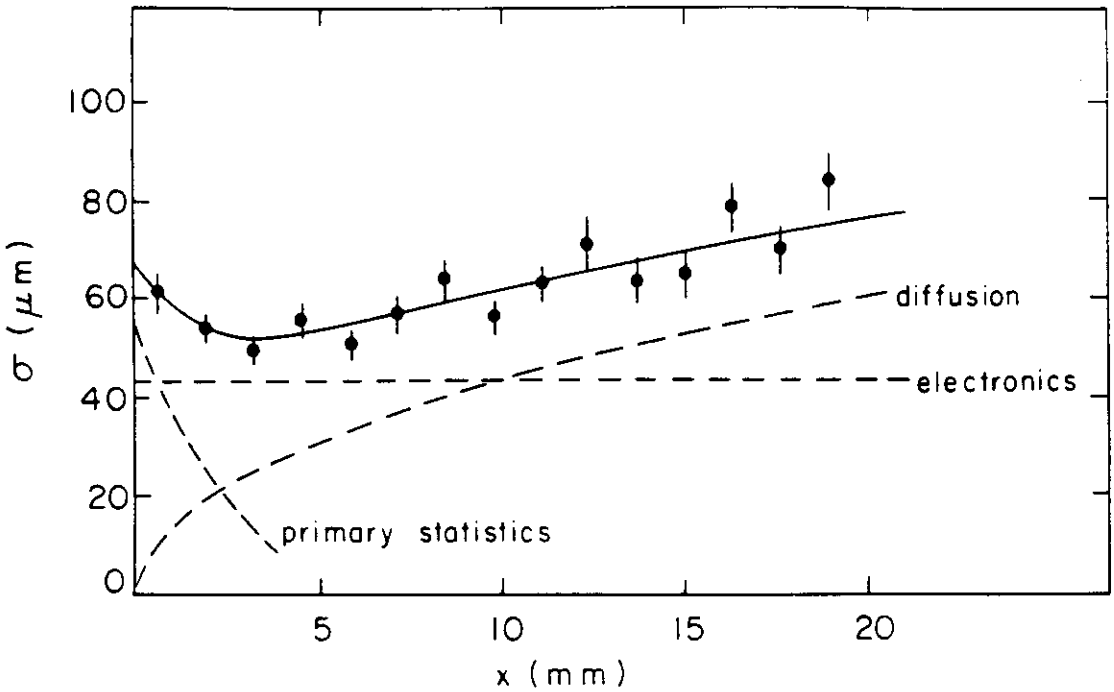

Fig. 6 Localization accuracy for high-energy charged particles measured in a drift chamber as a function of the distance from the wire. The various dispersive factors are also shown.

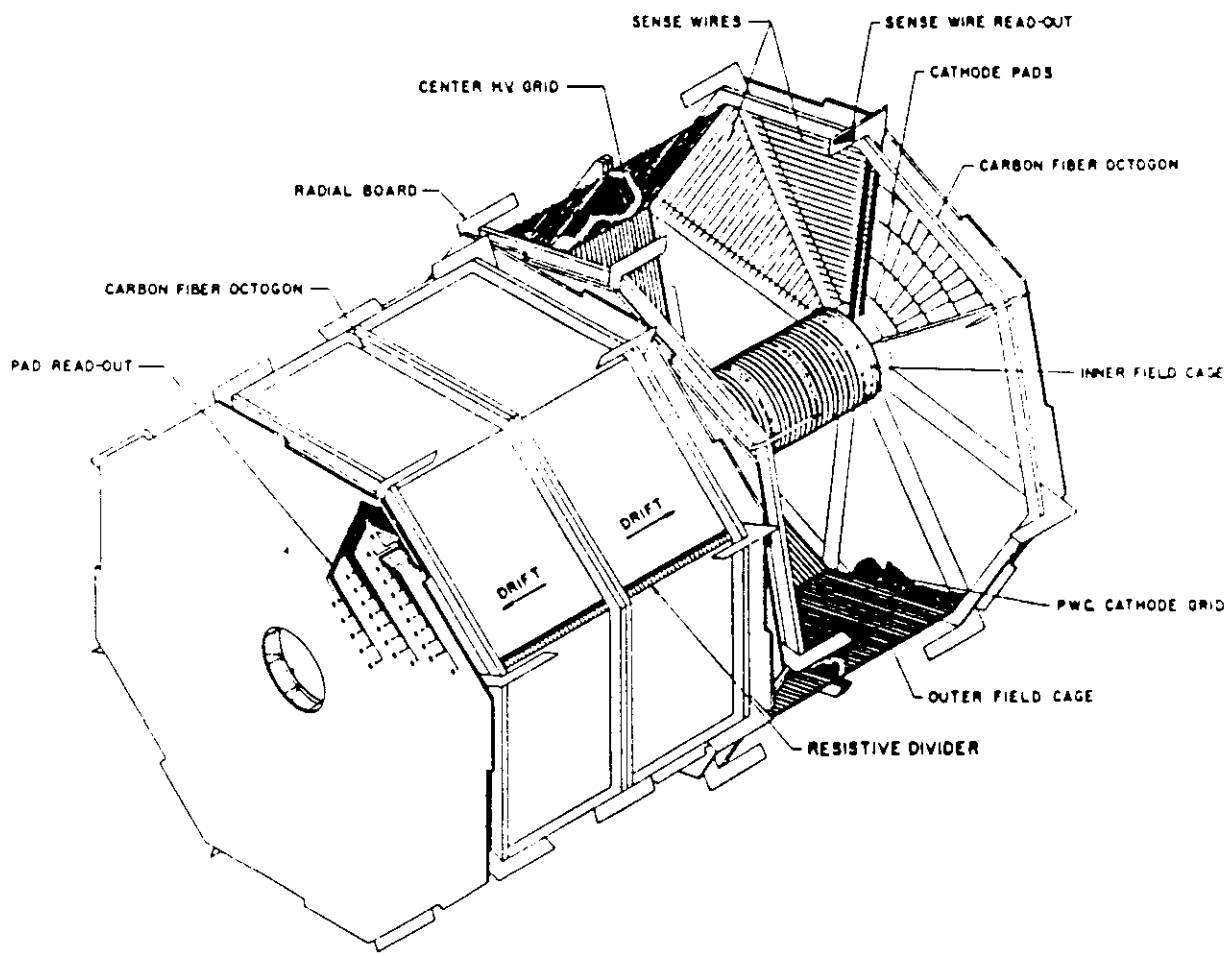

Fig. 7 Schematic view of a Time Projection Chamber. It is in fact made up of two individual cylindrical detectors, placed back to back; a thick drift region with a uniform electric field is followed by the multiplication and detection component (MWPC modules).

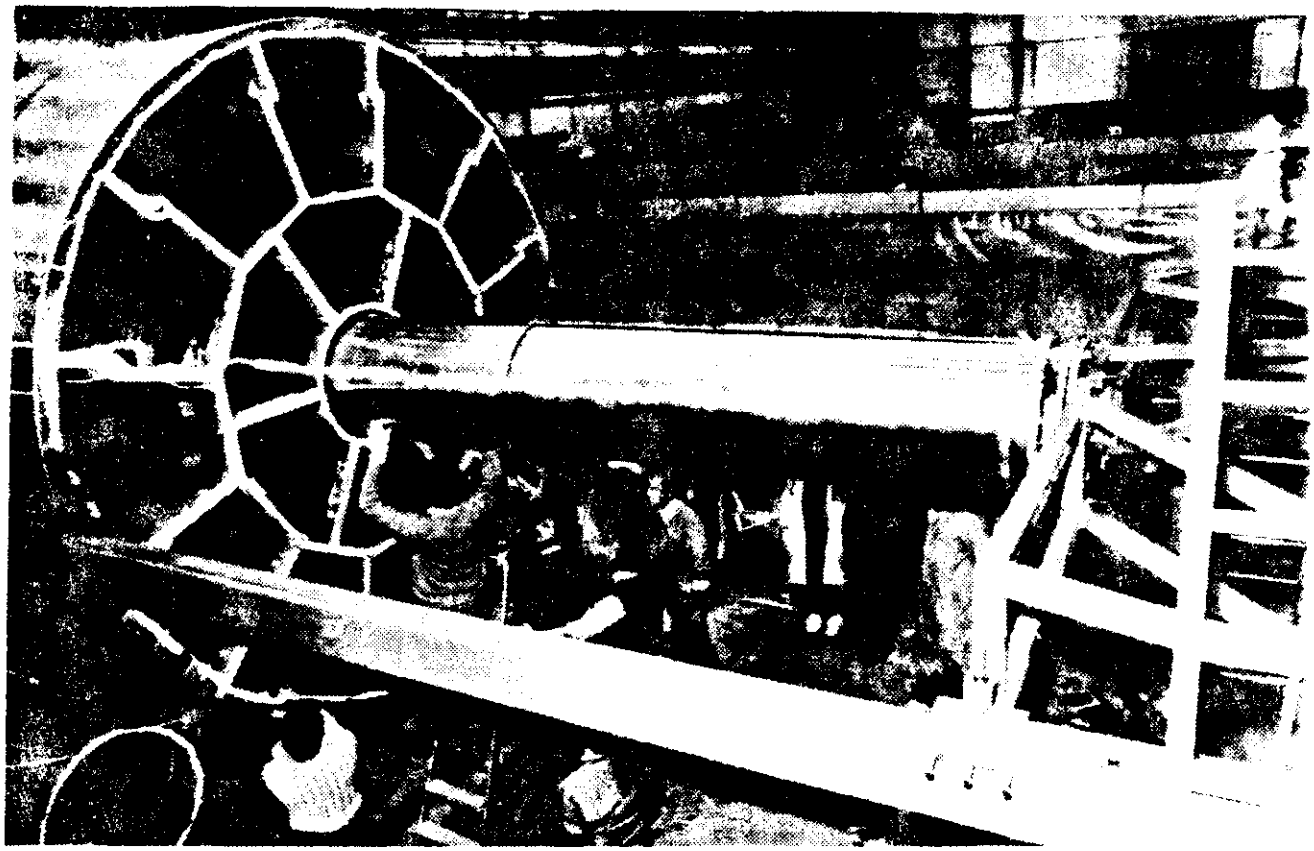

Fig. 8 Assembly of the TPC chamber of the ALEPH detector at CERN.

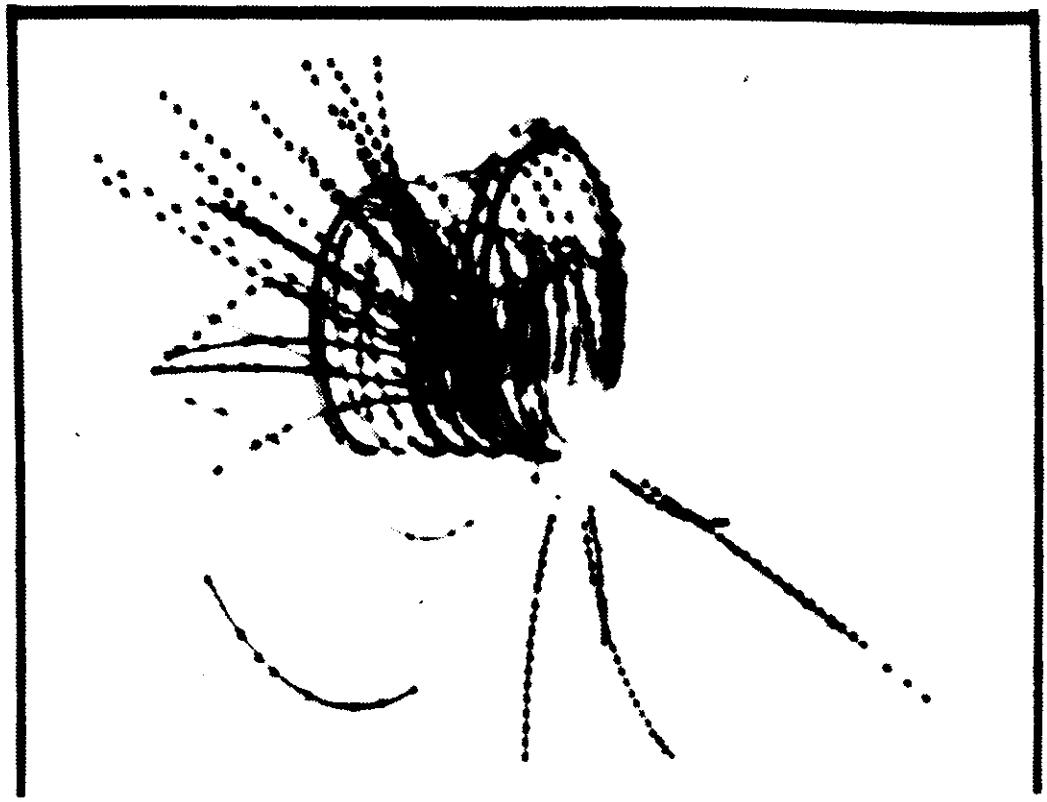

Fig. 9 Two-dimensional view of a simulated event in the ALEPH TPC. A low-energy electron is crossing the solenoidal magnetic field.

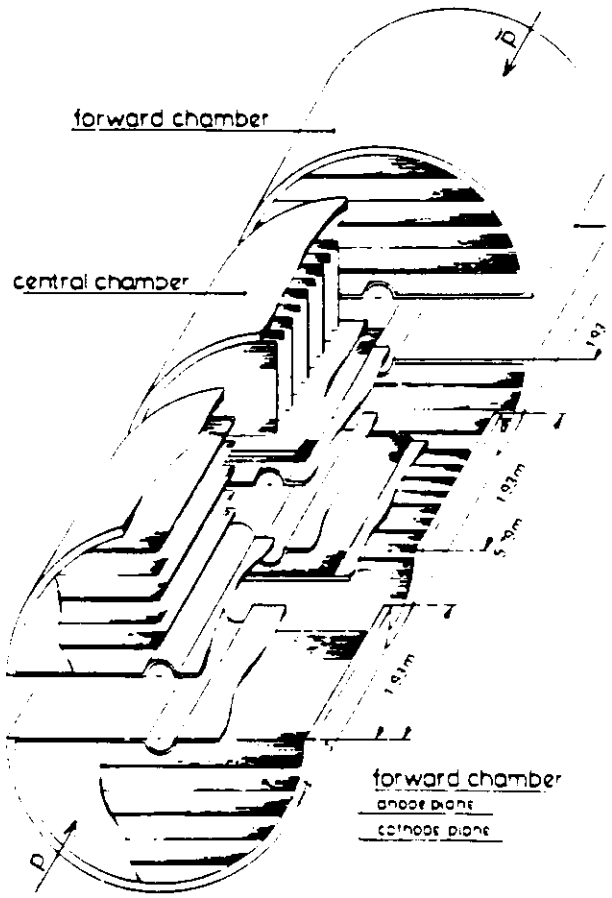

Fig. 10 Schematic view of the central detector of the UA1 experiment at the CERN $p\bar{p}$ Collider. It is made up of about 40 separate modules fitted around the vacuum tube of the machine and placed inside a magnet for momentum analysis.

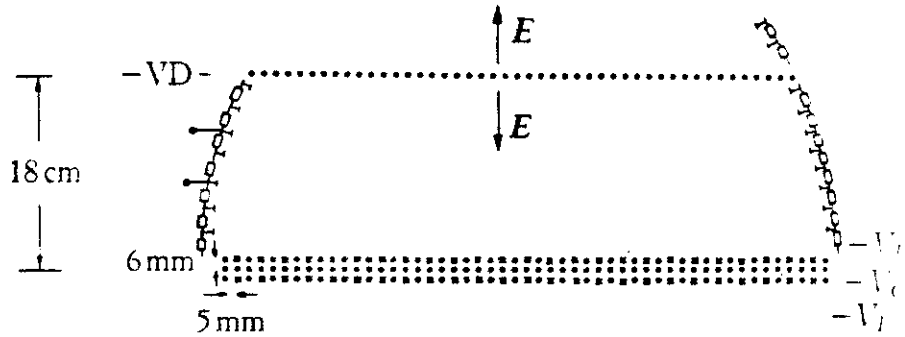

Fig. 11 Diagram of one of the drift chamber elements that make up the detector shown in the previous figure. The ionized tracks produced in the volume drift towards the detection area. Measurement of the drift-time and amplitude of the momentum at both ends of the wire provides the spatial coordinates of the track segment.

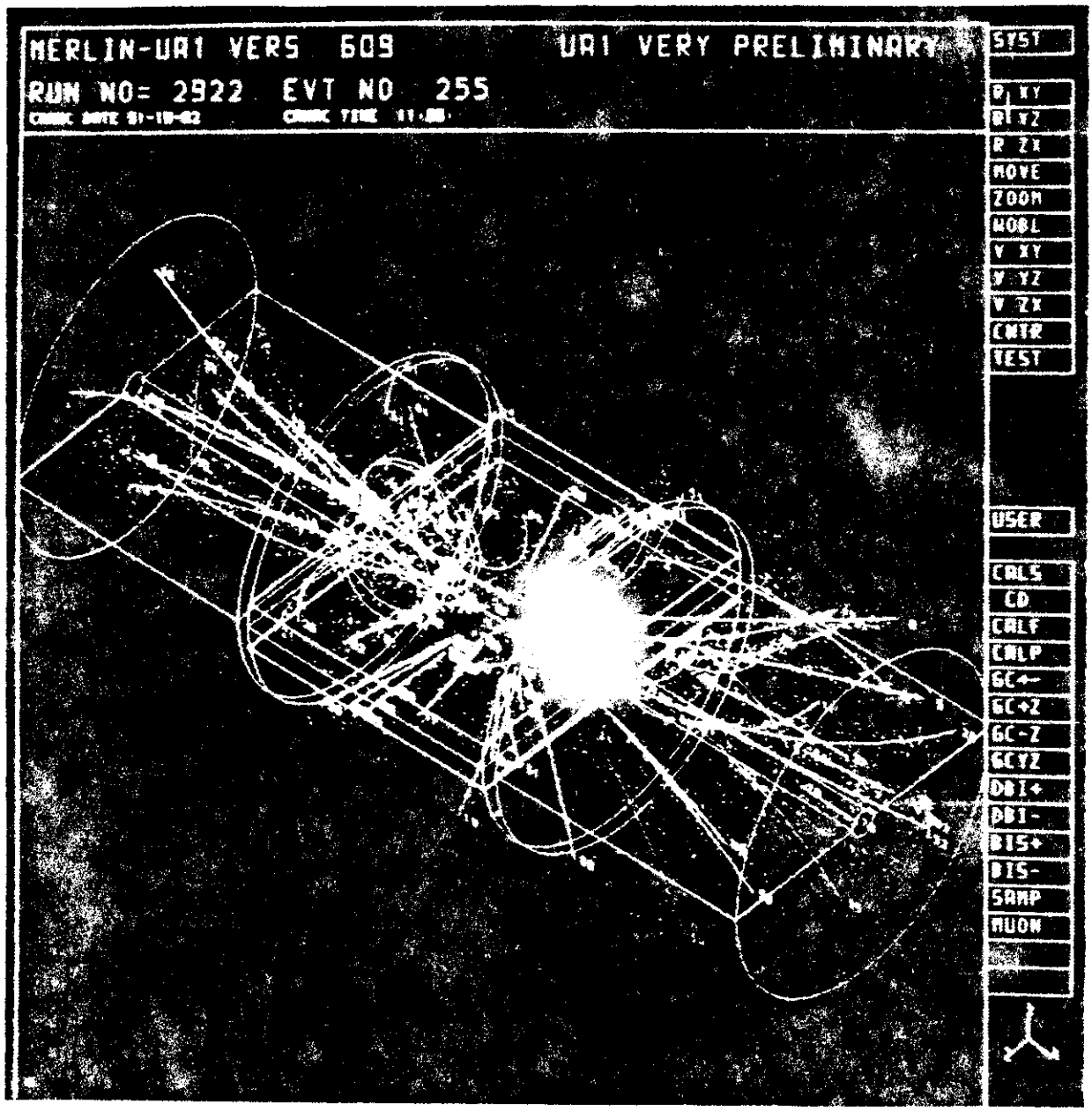

Fig. 12 A proton-antiproton interaction in the UA1 detector. The electronic image shows the charged tracks reconstructed using the measurement of the imaging chamber.

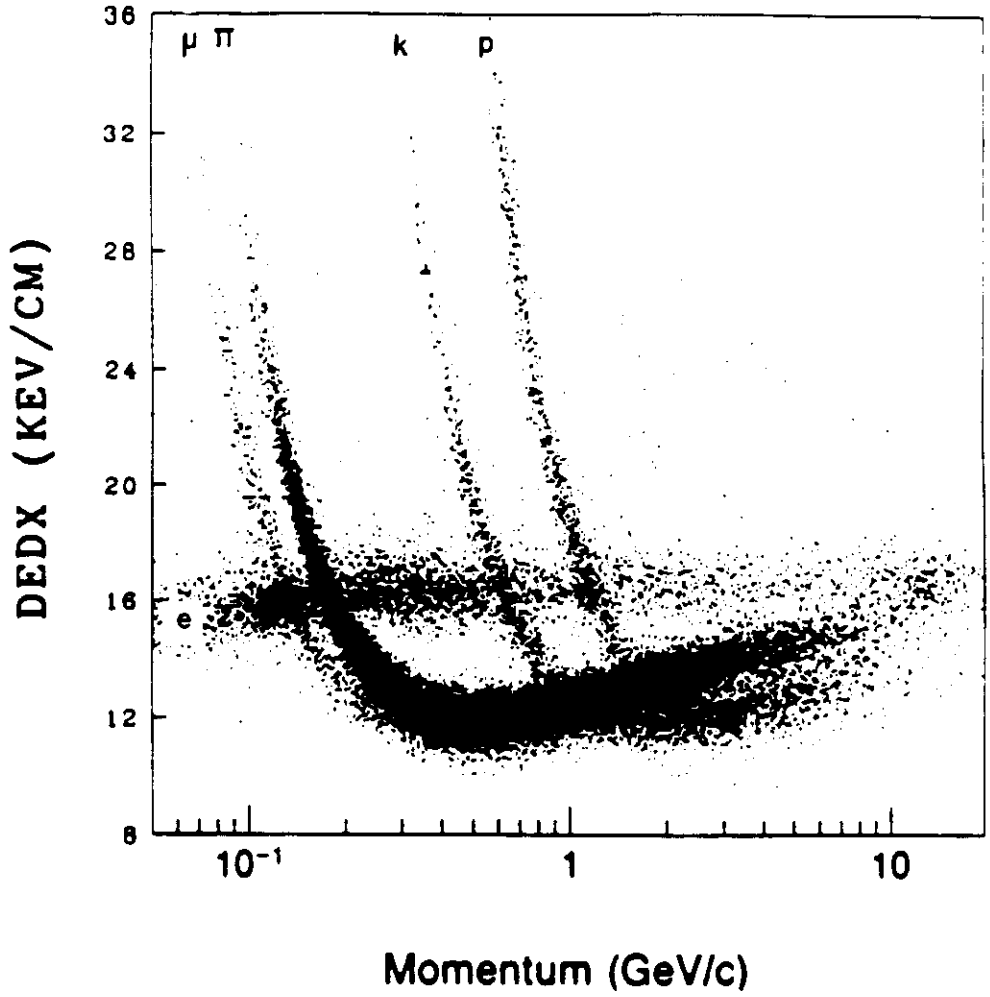

Fig. 13 Average differential energy loss measured as a function of momentum for fast charged particles in the Berkeley TPC. Particles of different mass can be very well identified in the low-momentum zone, and with less resolution in the relativistic rise region.

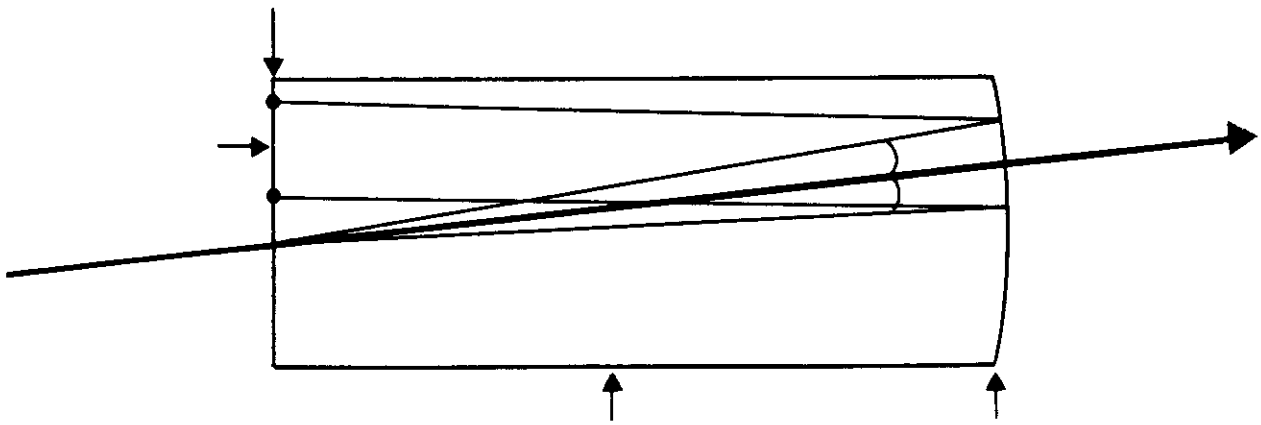

Fig. 14 Cherenkov ring detector. Photons emitted by Cherenkov effect by relativistic particles in the radiator at a constant angle are reflected by a spherical mirror as a circular image on the focal plane. The radius of the circle depends on the speed of the particle.

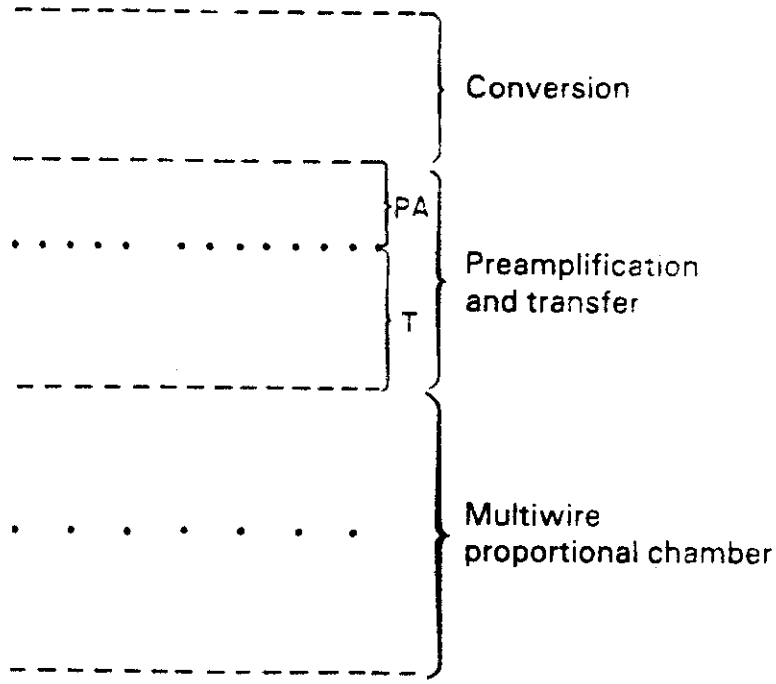

Fig. 15 Diagram of the multistep proportional chamber. A series of metal grids with varying potentials is used to cordon off a conversion region in which ionization takes place, a preamplification region where the initial charge is multiplied in a high field, and a MWPC which completes the amplification process. The structure makes it possible to attain high gains in a photosensitive gas; it is then used for the detection of isolated photoelectrons.

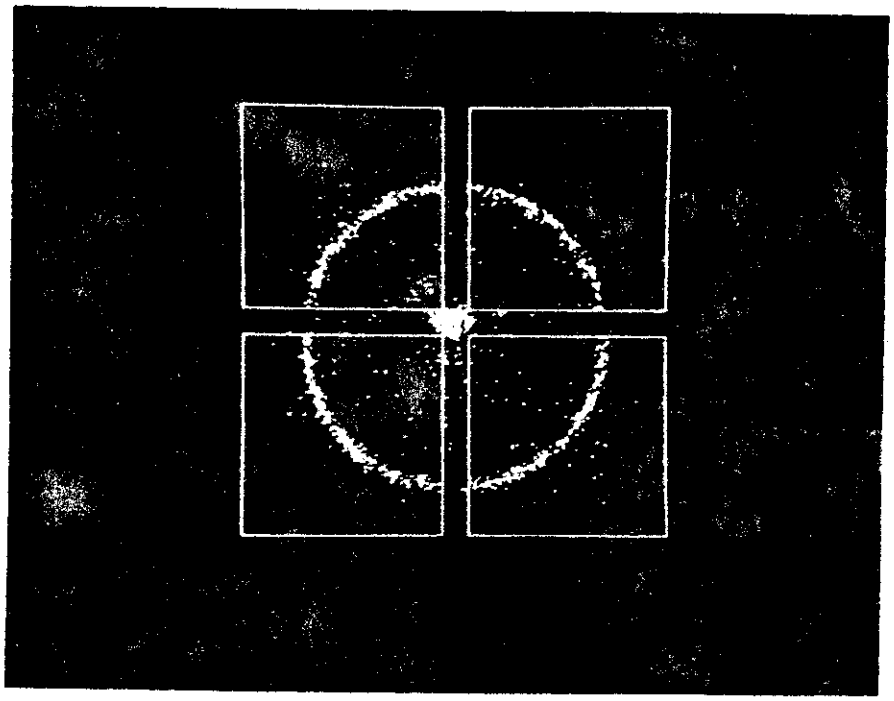

Fig. 16 Example of a Cherenkov ring obtained by superposing 100 collinear events. The photograph shows the outline of the four calcium fluoride crystals that are used as windows (each 10 cm × 10 cm). The particle beam is also detected and can be seen in the centre of the picture.

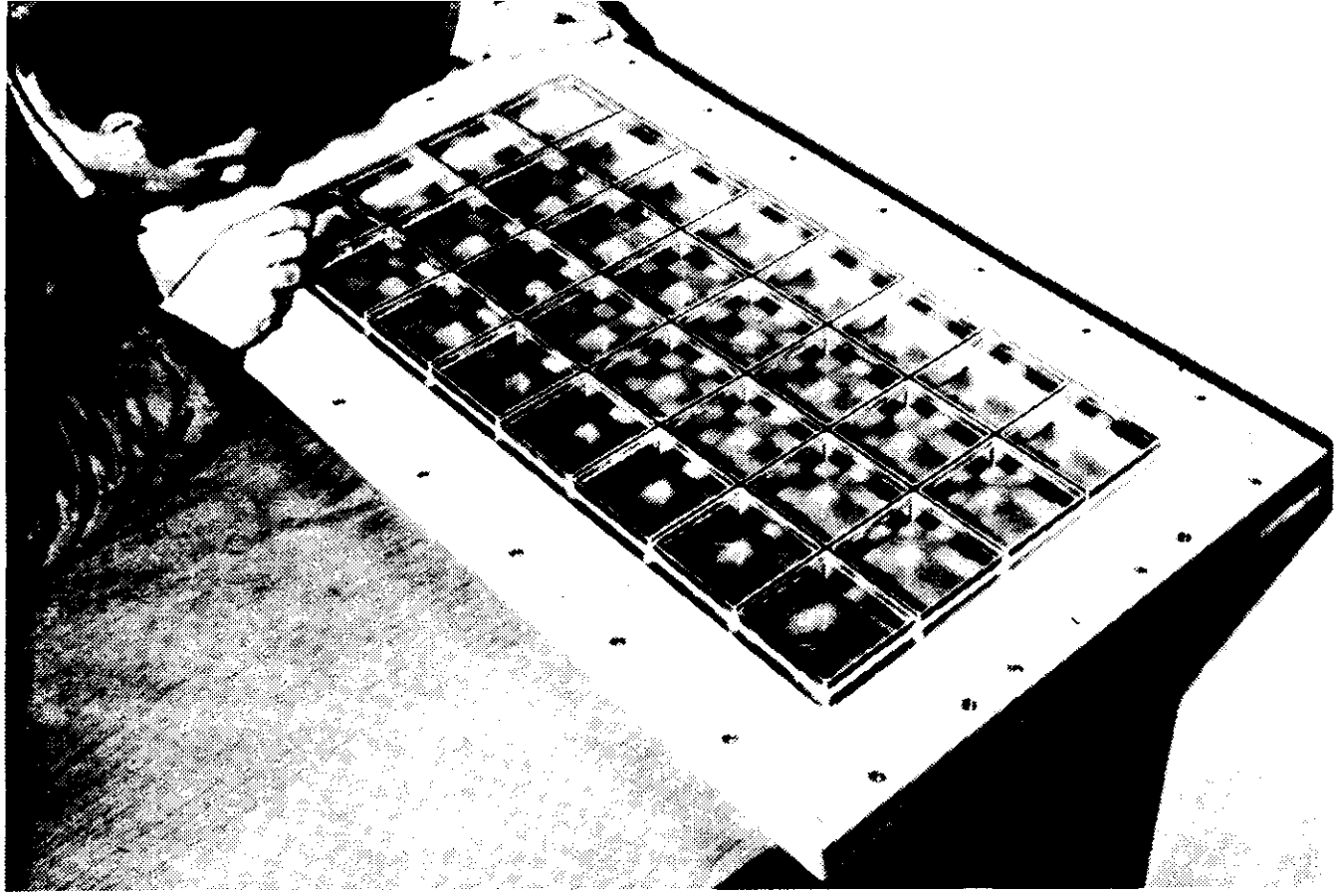

Fig. 17 Window made of 32 calcium fluoride crystals, made for a high-acceptance Cherenkov ring detector. Its fitting is particularly delicate because of the fragile nature of the crystals and the fact that it must form a tight seal between the photosensitive gas in the proportional chamber and the ultrapure gas of the radiator.

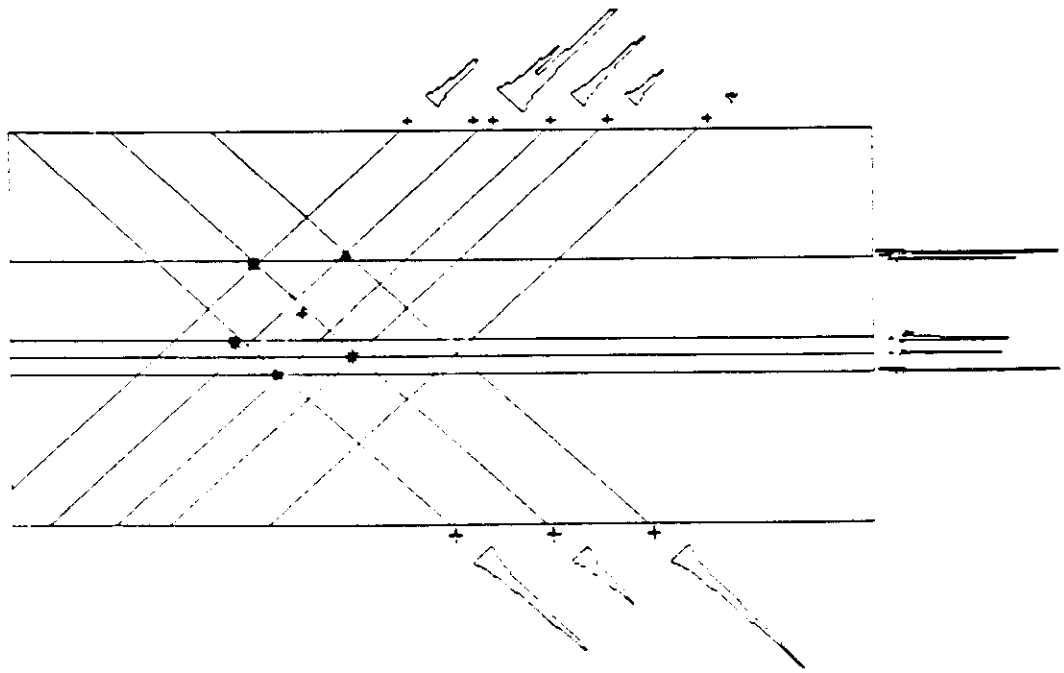

Fig. 18 A five-photon event appears like this in the analysis. The proportional chamber records the charge profiles induced on the two cathode planes and the anode plane, i.e. at three different angles. If the number of photons is not too high, their coordinates can be worked out without ambiguity.

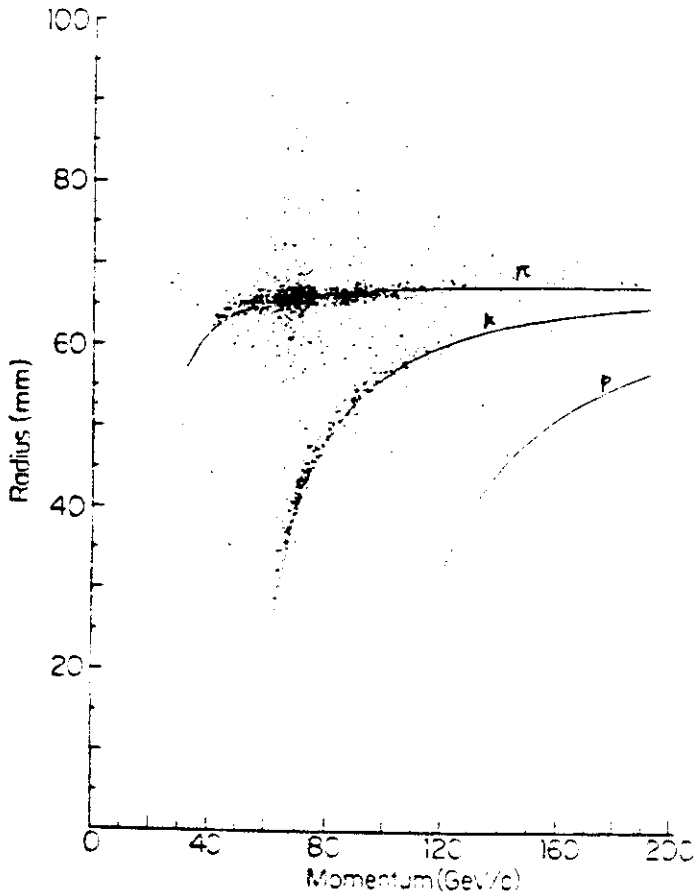

Fig. 19 Distribution of radii of the Cherenkov ring measured by particles with different masses as a function of their momentum. Within statistical limits, the μ and K ions are well separated up to high momenta.

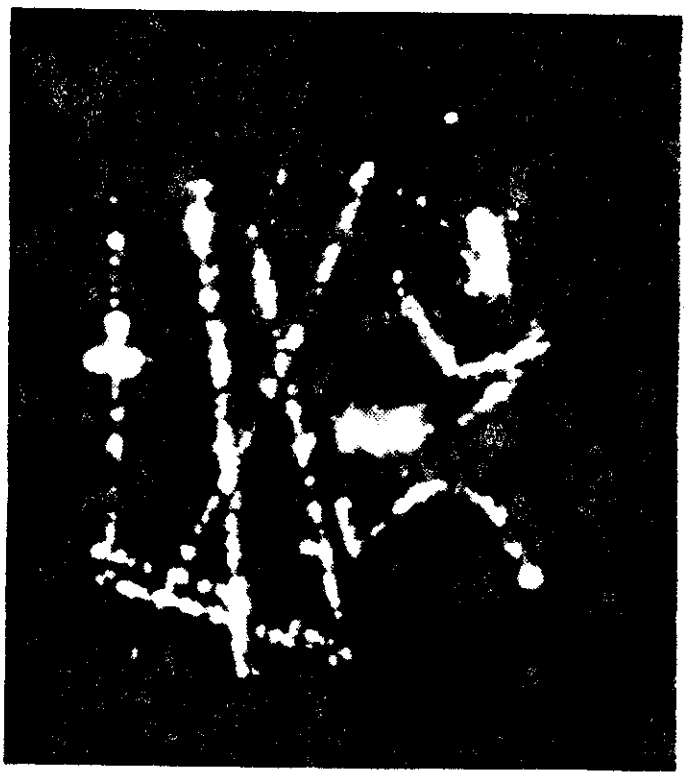

Fig. 20 Cosmic-ray tracks seen in an imaging chamber.

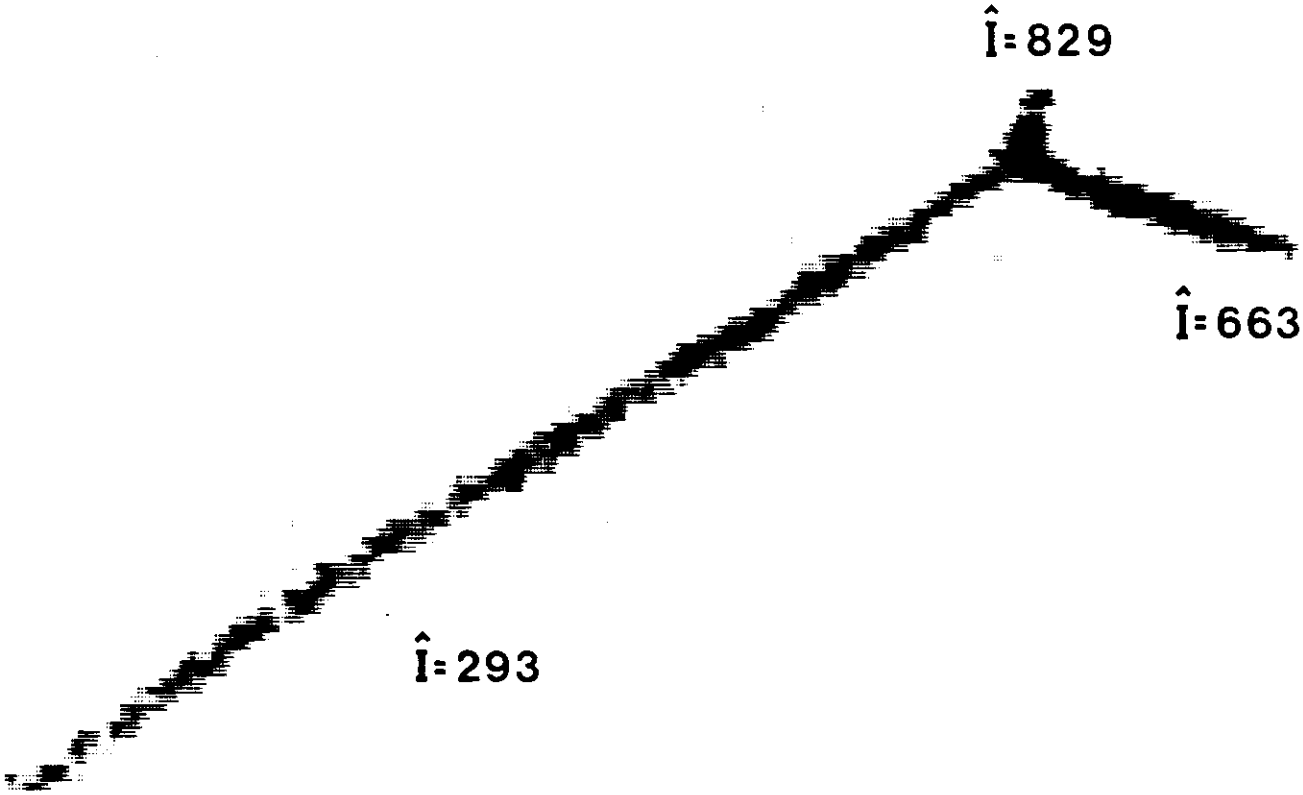

Fig. 21 An α-particle interacting with a helium nucleus, recorded with the imaging chamber; the numerical values on each segment indicate the light intensity recorded by the CCD camera, which corresponds to the loss of energy of the ions.

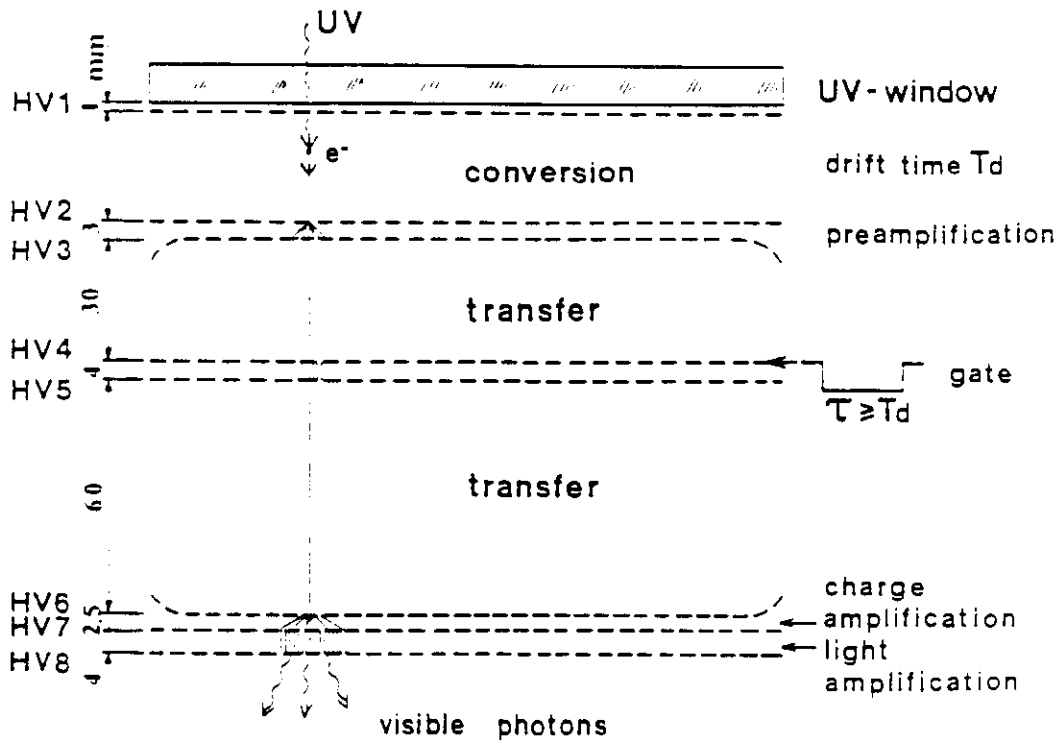

Fig. 22 A multistep chamber with an electronic gate used for detecting photons emitted by the Cherenkov effect.

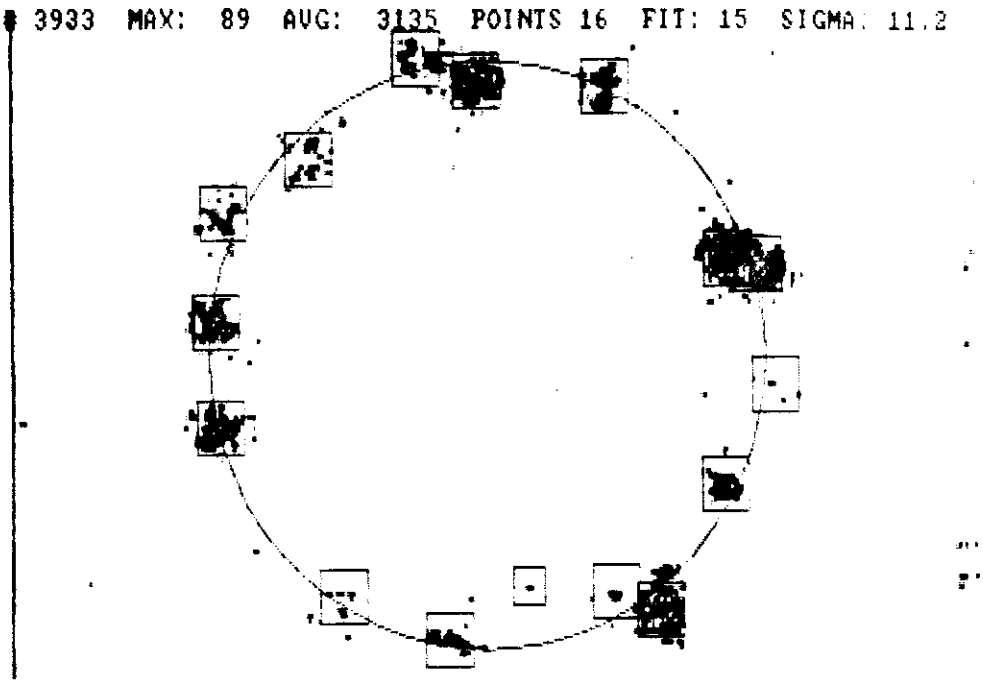

Fig. 23 An example of a Cherenkov ring with a dozen avalanches detected, each one corresponding to a photon.

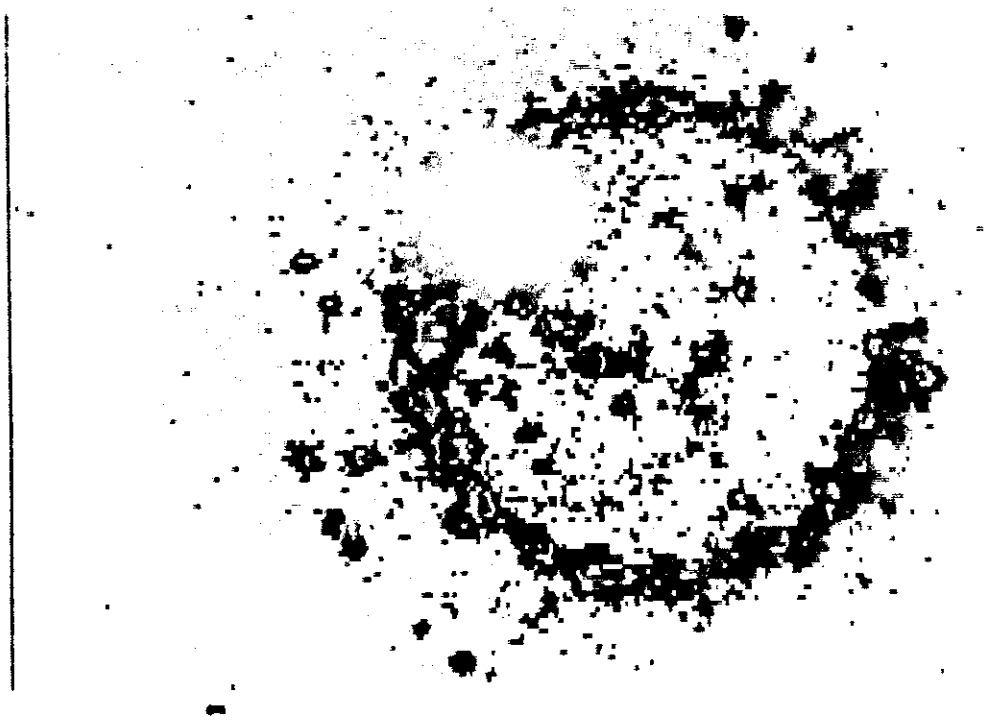

Fig. 24 Cherenkov ring produced by an electronic shower in a thick liquid radiator, and detected by the imaging chamber.

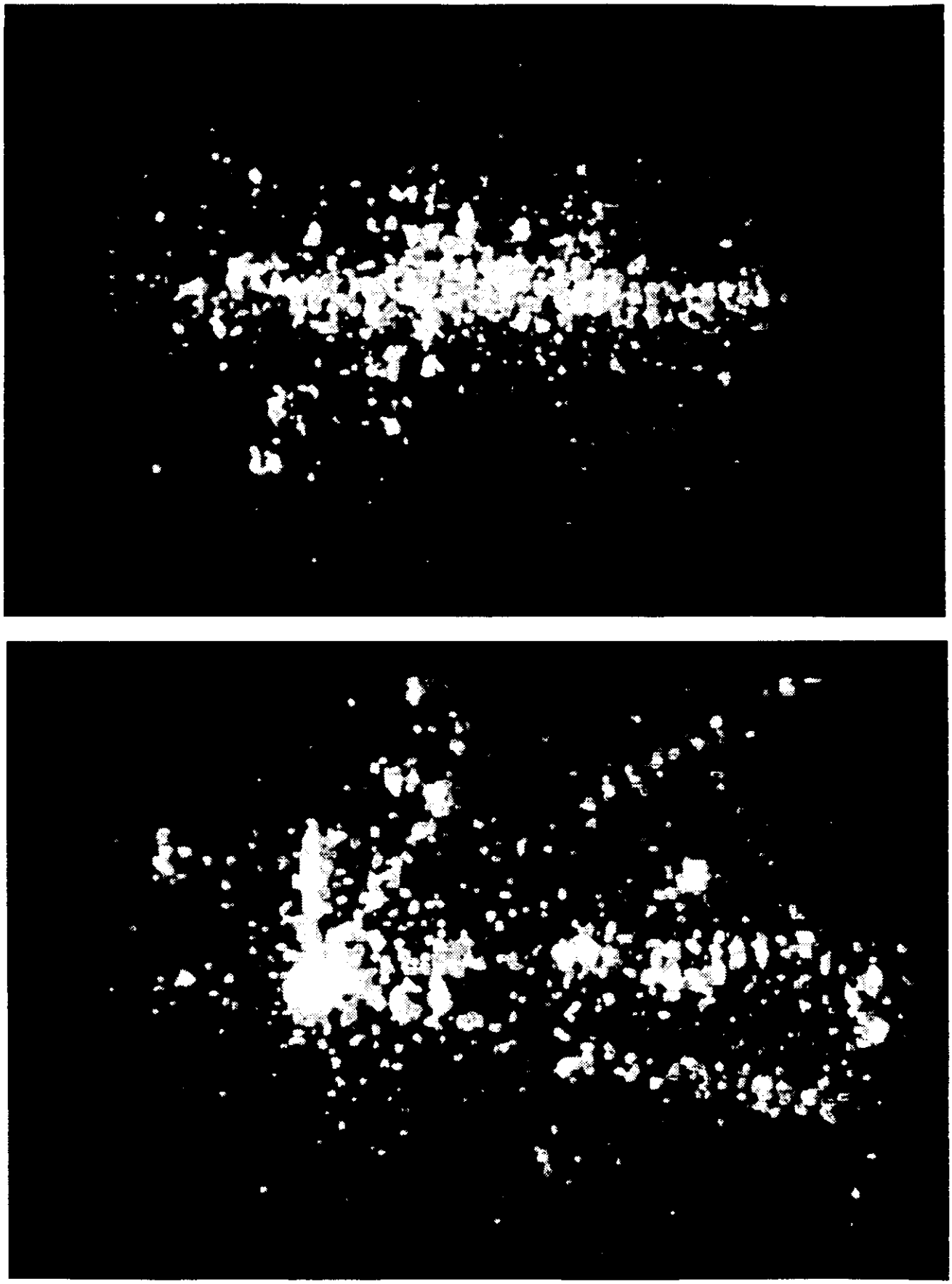

Fig. 25 An electromagnetic shower (top) and a hadron interaction seen in the high-density conversion imaging chamber.

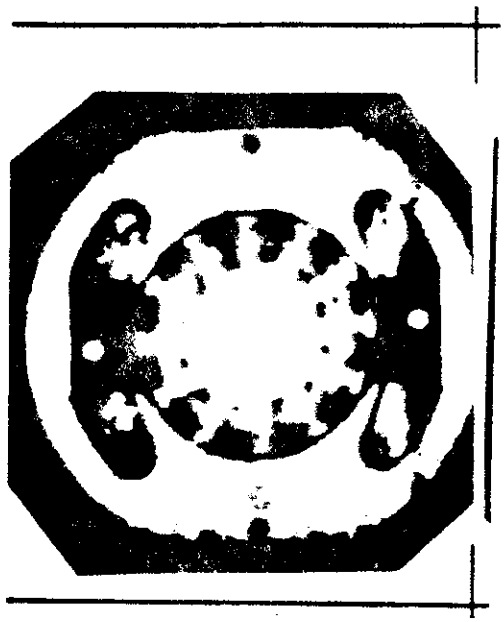

Fig. 26 One possible industrial application of fast-proton tomography: high-density materials (in the photograph, an electric motor) can be easily analysed. Synchronizing the data-taking with the rotor movement also makes it possible to take pictures in motion. (Photo CEN-Saclay).

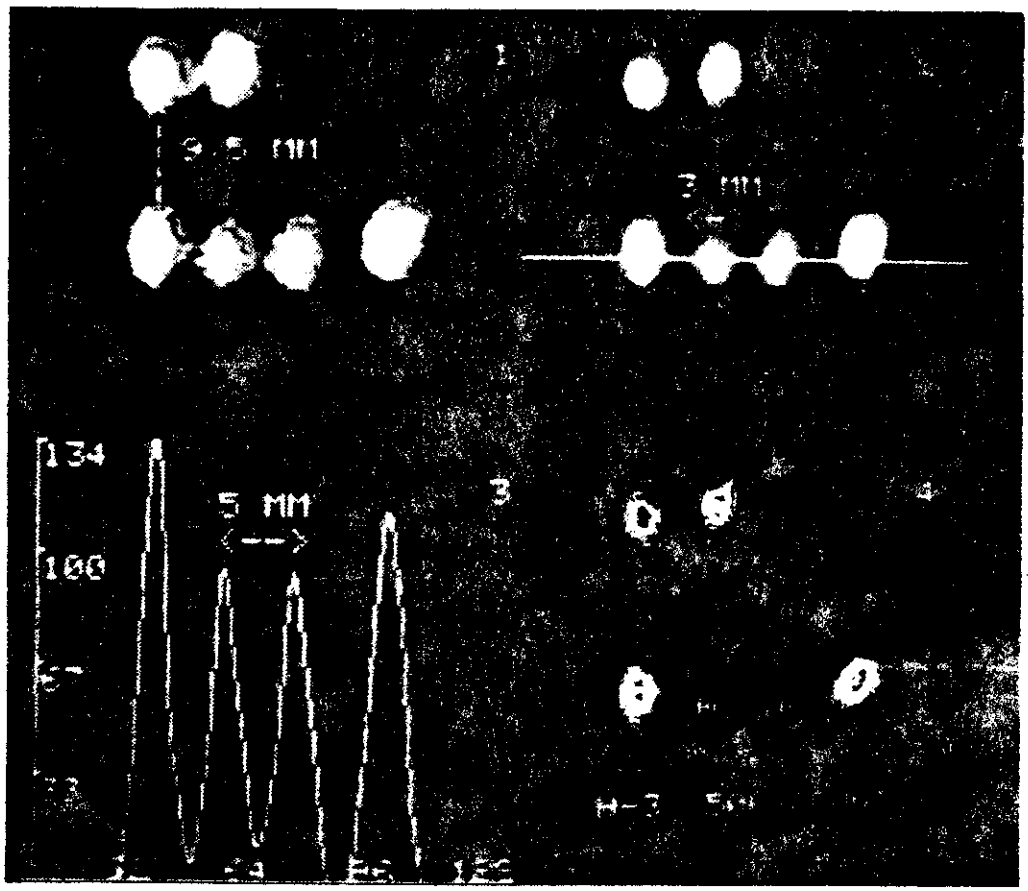

Fig. 27 Example of a digital autoradiograph of marked compounds obtained with a multiwire chamber. The upper part of the picture shows the distribution of activity before and after the application of a mathematical filter to improve the contrast. In the lower part, the projection of activity on a coordinate axis and the isometric distribution of the preparation are shown. (Photo INFN, Pisa)

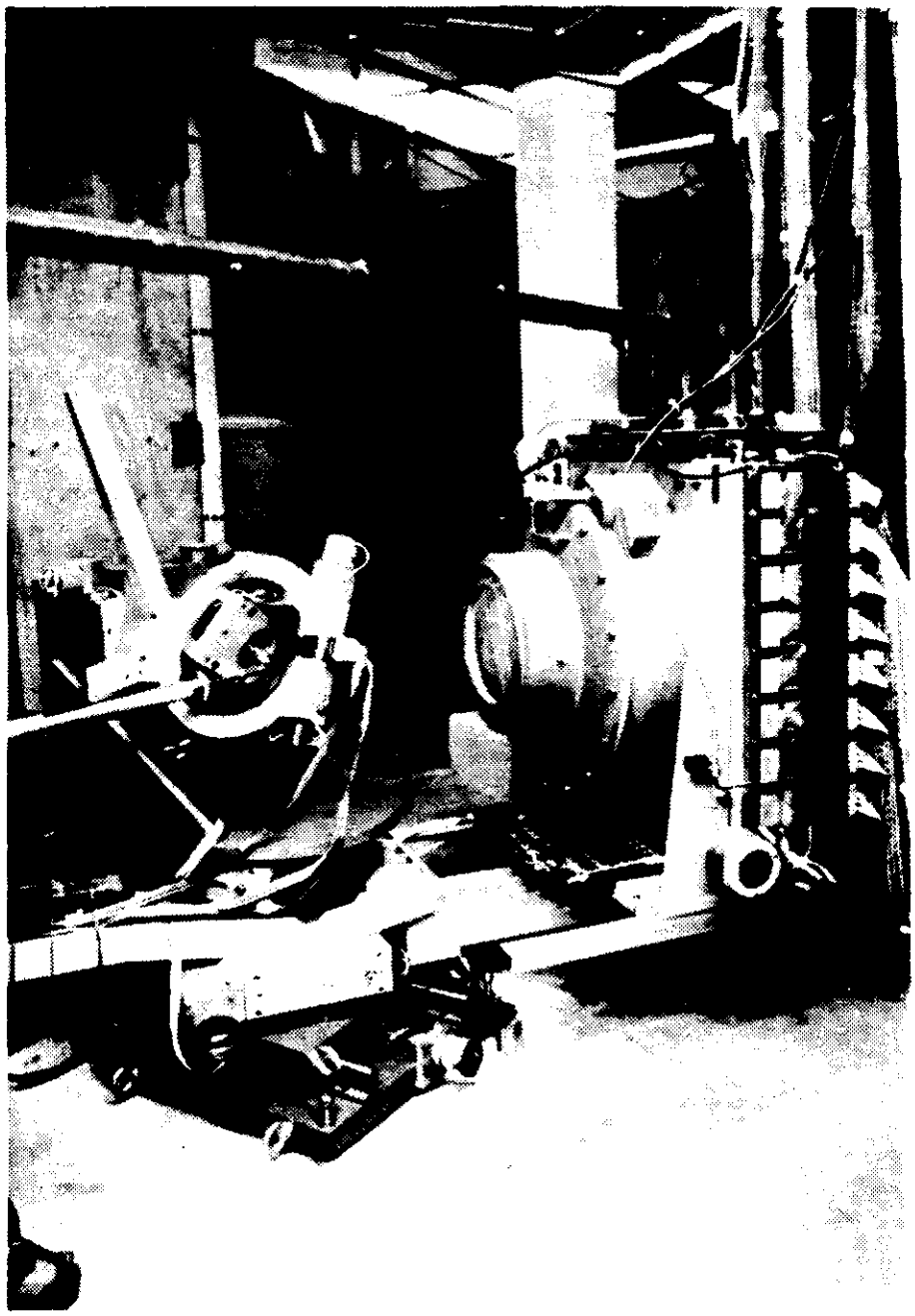

Fig. 28 The proportional chamber, with spherical conversion volume, used at Orsay for the structural analysis of the macromolecules of crystals. On the left can be seen the high-precision goniometer, which makes it possible to pivot the crystal struck by a monoenergetic beam of X-rays produced by the synchrotron radiation machine. (Photo LAL, Orsay)

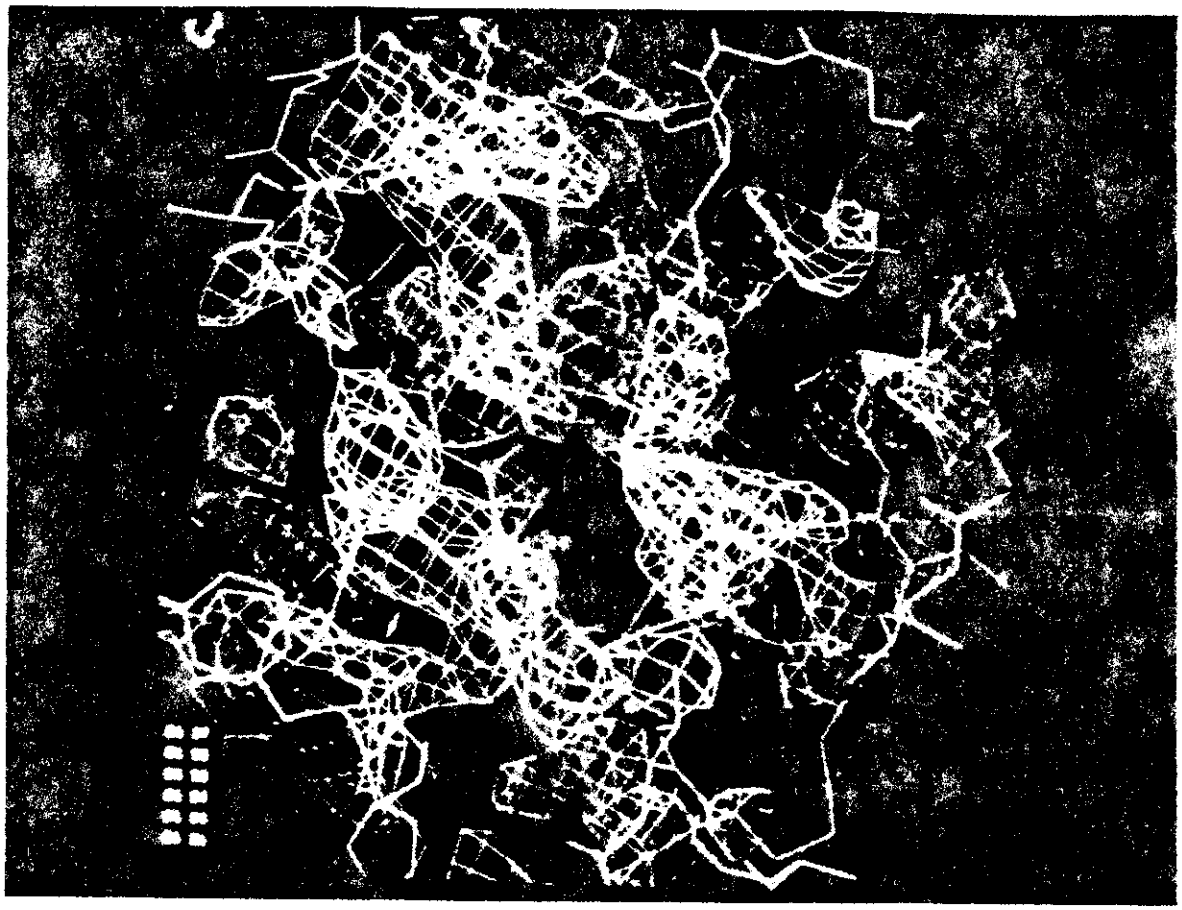

Fig. 29 Example of the electronic structure of a macromolecule reconstructed at Orsay using diffraction measurements carried out with the spherical chamber shown in the previous figure. (Photo LAL, Orsay)

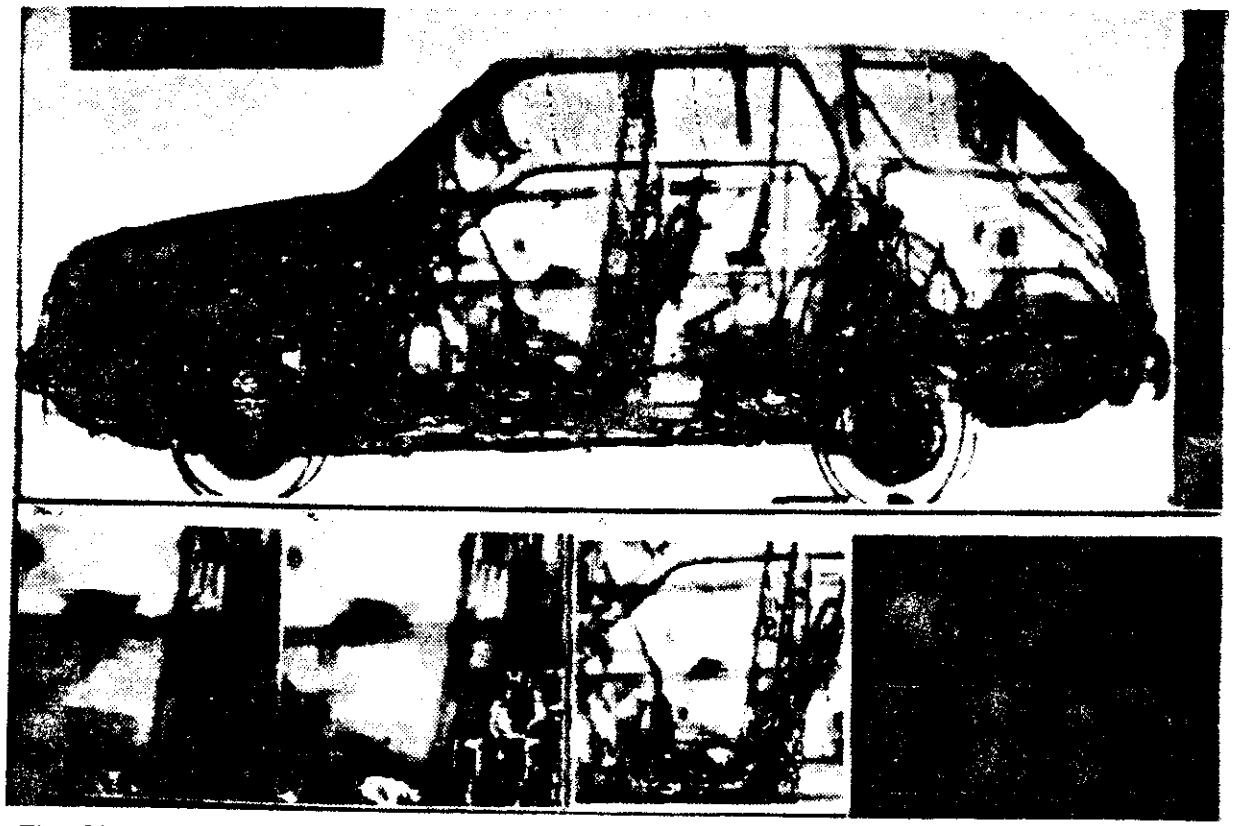

Fig. 30 Radiograph of a car made by the method based on the use of a multiwire proportional chamber with a thin converter and a grazing incidence of the hard-X-ray beam. (Photo Schlumberger)